Single-User Beamforming in Large-Scale MISO Systems with Per-Antenna Constant-Envelope Constraints: The Doughnut Channel

Saif Khan Mohammed* and Erik G. Larsson

arXiv:1111.3752v2 [cs.IT] 8 Jun 2012

Abstract

Large antenna arrays at the transmitter (TX) has recently been shown to achieve remarkable intra-cell interference suppression at low complexity. However, building large arrays in practice, would require the use of power-efficient RF amplifiers, which generally have poor linearity characteristics and hence would require the use of input signals with a very small peak-to-average power ratio (PAPR). In this paper, we consider the single-user Multiple-Input Single-Output (MISO) channel for the case where the TX antennas are constrained to transmit signals having constant envelope (CE). We show that, with per-antenna CE transmission the effective channel seen by the receiver is a SISO AWGN channel with its input constrained to lie in a doughnut-shaped region. For a broad class of fading channels, analysis of the effective doughnut channel shows that under a per-antenna CE input constraint, i) compared to an average-only total TX power constrained MISO channel, the extra total TX power required to achieve a desired information rate is small and bounded, ii) with N TX antennas an $O(N)$ array power gain is achievable, and iii) for a desired information rate, using power-efficient amplifiers with CE inputs would require significantly less total TX power when compared to using highly linear (power-inefficient) amplifiers with high PAPR inputs.

Index Terms

Beamforming, MISO, constant envelope, per-antenna.

The authors are with the Communication Systems Division, Dept. of Electrical Engineering (ISY), Linköping University, Linköping, Sweden. This work was supported by the Swedish Foundation for Strategic Research (SSF) and ELLIIT. E. G. Larsson is a Royal Swedish Academy of Sciences (KVA) Research Fellow supported by a grant from the Knut and Alice Wallenberg Foundation. Parts of the results in this paper will be presented at IEEE ICC 2012.

I. INTRODUCTION

The high electrical power consumption in cellular base stations (BS) has been recognized as a major problem worldwide [1]. One way of reducing the power consumed is to reduce the total radiated radio-frequency (RF) power. In theory, the total radiated power from a BS can be reduced without affecting the downlink throughput, by increasing the number of antennas. This effect has been traditionally referred to as the "array power gain" [2]. In addition to improving power-efficiency, there has been a great deal of recent interest in multi-user Multiple-Input Multiple-Output (MIMO) systems with *large antenna arrays* [3], [4], due to their ability to substantially reduce intra-cell interference with very simple signal processing. In general, multiple antenna beamforming is a well known technology to improve link performance [5].

To illustrate the improvement in power efficiency with large antenna arrays, let us consider a MISO channel between a transmitter (TX) having $N > 1$ antennas and a single-antenna receiver. With knowledge of the channel vector ($\mathbf{h} = (h_1, h_2, \cdots, h_N)^T$) at the TX and an *average-only* total transmit power constraint of P_T, an information symbol u (with mean energy $\mathbb{E}[|u|^2] = 1$) can be beamformed in such a way (the i-th antenna transmits $\sqrt{P_T} h_i^* u / \|\mathbf{h}\|_2$) that the signals from different TX antennas add up *coherently* at the receiver (the received signal is $\sqrt{P_T}\|\mathbf{h}\|_2 u$), thereby resulting in an effective channel with a received signal power that is $\|\mathbf{h}\|_2^2/|h_1|^2$ times higher compared to a scenario where the TX has only one antenna. For a broad class of fading channels (e.g., i.i.d. fading, single-path direct-line-of-sight (DLOS)) $\|\mathbf{h}\|_2^2 = |h_1|^2 O(N)$, and therefore, for a fixed desired received signal power, the total transmit power can be reduced by roughly half with every doubling of the number of TX antennas. This type of beamforming is referred to as "Maximum Ratio Transmission" (MRT) (see Fig. 1(a)).

In theory, to achieve an order of magnitude reduction in the total radiated power (without affecting throughput) we would need TX with a large number of antennas (by large, we mean tens or even hundreds [3], [4]). However, building very large arrays in practice requires that each individual antenna, and its associated RF electronics, be cheaply manufactured and implemented in power-efficient technology. It is known that conventional BS are *highly power-inefficient*. Typically, the ratio of radiated power to the total power consumed is less than 5 percent, the main reason being the use of highly *linear* and power-inefficient analog devices like the power amplifier [6].[2] Generally, high linearity implies low power efficiency and

[2]In a conventional BS, about $40 - 50$ percent of the total operational power is consumed by the power amplifier and the associated RF electronics, which have a power efficiency of only about $5 - 10$ percent [6].

vice-versa. Therefore, non-linear but highly power-efficient amplifiers must be used. With non-linear power amplifiers, the signal transmitted from each antenna must have a *low peak-to-average-power-ratio*, so as to avoid significant signal distortion. The type of signal that facilitates the use of the most power-efficient and cheap power amplifiers/analog components is therefore a *constant envelope* (CE) signal.

With this motivation, in this paper, we consider a single-user Gaussian MISO fading channel with the signal transmitted from each TX antenna constrained to have a constant envelope. Fig. 1(b) illustrates the proposed signal transmission under a per-antenna CE constraint. Essentially, for a given information symbol u to be communicated to the single-antenna receiver, the signal transmitted from the i-th antenna is $\sqrt{P_T/N}e^{j\theta_i^u}$. The transmitted phase angles $(\theta_1^u, \cdots, \theta_N^u)$ are determined in such a way that the noise-free signal received matches closely with u. The amplitude of the signal transmitted from each antenna is *constant* and equal to $\sqrt{P_T/N}$ for every channel-use, irrespective of the channel realization. By way of contrast, with MRT, the amplitude of the transmitted signal *depends upon the channel realization* as well as on u, and can vary from 0 to $\sqrt{P_T}|u|$. Since the CE constraint is much more *restrictive* than the average-only total power constraint in MRT, a natural question which arises now is how much array power gain can be achieved with the per-antenna CE constraint. Also, compared to MRT, how much extra total transmit power is required with per-antenna CE transmission to achieve a given information rate?

So far, in the open literature, these questions have not been addressed. For the special case of $N = 1$ (SISO AWGN), the channel capacity under a CE input constraint has been reported in [7]. However for $N > 1$, known reported works on per-antenna power constrained communication consider an average-only or peak-only power constraint [8]–[13]. For the single-user scenario, in [8], the author considers the problem of finding the optimal transmit and receive matrices which maximize the received signal-to-noise-and-interference-ratio (SINR) in a MIMO channel, subject to a per-antenna average power constraint at the TX. In [9], the author has derived a closed-form expression for the capacity of a single-user MISO channel with a per-antenna average power constraint at the TX. In [10], the authors compute bounds on the capacity of a noncoherent single-user MIMO channel with peak per-antenna power constraints at the TX.

For the multiuser MIMO broadcast channel with per-antenna power constraints, in [11] the authors consider minimization of the per-antenna average power radiated by the transmitter subject to a minimum SINR constraint for each user in the downlink. They propose efficient numerical methods for solving this

problem using uplink-downlink duality. In [12], the authors study the optimal multi-user linear zero-forcing beamformer which maximizes the minimum information rate to the downlink users, under per-antenna average power constraints at the BS. In [13], the authors consider the scenario where users can also have multiple antennas, and propose methods to maximize the weighted sum-rate and max-min rate under a per-antenna average power constraint at the BS.

In contrast to the above works on per-antenna *average/peak* power constrained communication, in this paper, we consider the more stringent per-antenna constant-envelope constraint where each antenna emits a signal of *constant* amplitude $\sqrt{P_T/N}$.

The specific contributions presented in this paper are: i) we show that, under a per-antenna CE constraint at the TX, the MISO channel reduces to a SISO AWGN channel with the noise-free received signal being constrained to lie in a "doughnut" shaped region in the complex plane, ii) using the equivalent doughnut channel model, we derive analytical upper and lower bounds on the MISO channel capacity under per-antenna CE transmission, iii) under per-antenna CE transmission, for large N we show that the optimal information alphabet (in terms of achieving capacity) is discrete-in-amplitude and uniform-in-phase, and iv) we also propose novel algorithms for transmit precoding under the per-antenna CE constraint. Our analysis shows that for a large class of fading channels (i.i.d. Rayleigh fading, i.i.d. fading channels where the channel gains are bounded[3], DLOS), i) under the per-antenna CE constraint, an array power gain of $O(N)$ is indeed achievable with N antennas, ii) for a desired information rate to be achieved, compared to the MRT precoder with an average-only total transmit power constraint, the extra total transmit power required under per-antenna CE transmission is small and bounded, iii) by using a sufficiently large antenna array, at high total transmit power P_T, the ratio of the information rate achieved under the per-antenna CE constraint to the capacity of the average-only total transmit power constrained MISO channel can be guaranteed to be *close to* 1, with high probability. This stands in contrast to Wyner's result in [7] for $N = 1$, where this ratio is *only* $1/2$ at high P_T. Analytical results are supported with numerical results for the i.i.d. Rayleigh fading channel. The analysis and algorithms presented are general and applicable to systems with any number of transmit antennas.

Notation: $\mathbb{C}$ and $\mathbb{R}$ denote the set of complex and real numbers. $|x|$, x^* and $\arg(x)$ denote the absolute value, complex conjugate and argument of $x \in \mathbb{C}$ respectively. For any positive $p \geq 1$, $\|\mathbf{h}\|_p \triangleq (\sum_i |h_i|^p)^{1/p}$

[3]In practice, real-world channels generally have bounded channel gains.

denotes the Euclidean p-norm of $\mathbf{h} = (h_1, \cdots, h_N) \in \mathbb{C}^N$. $\mathbb{E}[\cdot]$ denotes the expectation operator. $\log(\cdot)$ denotes the natural logarithm, and $\log_2(\cdot)$ denotes the base-2 logarithm. Abbreviations: r.v. (random variable), bpcu (bits-per-channel-use), p.d.f. (probability density function).

II. System model

We consider a single-user MISO system. The complex channel gain between the i-th transmit antenna and the single antenna receiver is denoted by h_i, and the total channel vector is denoted by $\mathbf{h} = (h_1, h_2, \cdots, h_N)^T$. TX is assumed to have perfect knowledge[4]of $\mathbf{h}$, whereas the receiver is required to have only partial knowledge (we shall discuss this later in more detail). Let the complex symbol transmitted from the i-th antenna be denoted by x_i. The complex symbol received is

$$y = \sum_{i=1}^{N} h_i x_i + w \tag{1}$$

where w denotes the circularly symmetric AWGN having mean zero and variance σ^2, i.e., $\mathcal{CN}(0, \sigma^2)$. Due to the CE constraint on each antenna and assuming a total transmit power constraint of P_T, we must have $|x_i|^2 = P_T/N$, $i = 1, \ldots, N$. Therefore x_i must be of the form

$$x_i = \sqrt{\frac{P_T}{N}} e^{j\theta_i} \ , \ i = 1, 2, \ldots, N \tag{2}$$

where $j \triangleq \sqrt{-1}$, and $\theta_i \in [-\pi \, , \, \pi)$ is the phase of x_i. We refer to the type of signal transmission in (2) as "CE transmission". Note that under an average-only total transmit power constraint, the transmitted signals are *only* required to satisfy $\mathbb{E}[\sum_i |x_i|^2] = P_T$, which is much less restrictive than (2). Under CE transmission, the signal received is given by (using (1) and (2))

$$y = \sqrt{\frac{P_T}{N}} \sum_{i=1}^{N} h_i e^{j\theta_i} + w. \tag{3}$$

Let $\Theta \triangleq (\theta_1, \theta_2, \cdots, \theta_N)^T$ denote the vector of transmitted phase angles and let $u \in \mathcal{U} \subset \mathbb{C}$ denote the information symbol to be communicated to the receiver, where $\mathcal{U}$ is the information symbol alphabet. For a given u, the precoder in the transmitter uses a map $\Phi(\cdot) : \mathcal{U} \to [-\pi, \pi)^N$ to generate the transmit phase

[4]For large N, with Time-Division-Duplex (TDD) communication and assuming a reciprocal channel, channel measurements at the TX using reverse link pilot signals can be used to estimate the forward channel. A preliminary study done by us reveals that, the performance of the proposed CE transmission scheme degrades with increasing estimation error variance. However, interestingly, with i.i.d. Rayleigh fading the performance loss is small even when the standard deviation of the estimation error is of the same order as the average channel gain.

angle vector, i.e., $\Theta = \Phi(u)$. Let the set of possible noise-free received signals scaled down by $\sqrt{P_T}$, i.e., $\sqrt{\frac{1}{N}}\sum_{i=1}^{N} h_i e^{j\theta_i}$, be given by

$$\mathcal{M}(\mathbf{h}) \triangleq \left\{ \frac{\sum_{i=1}^{N} h_i e^{j\theta_i}}{\sqrt{N}} \ , \ \theta_i \in [-\pi, \pi) \ i = 1, \ldots, N \right\} \tag{4}$$

By choosing $\mathcal{U} \subseteq \mathcal{M}(\mathbf{h})$, for any $u \in \mathcal{U}$, it is implied that $u \in \mathcal{M}(\mathbf{h})$, and therefore from (4) it follows that, there exists a phase angle vector $\Theta^u = (\theta_1^u, \cdots, \theta_N^u)$ such that[5]

$$u = \sqrt{\frac{1}{N}} \sum_{i=1}^{N} h_i e^{j\theta_i^u}. \tag{5}$$

With the precoder map

$$\Phi(u) \triangleq \Theta^u \tag{6}$$

where Θ^u satisfies (5), the received signal is given by

$$y = \sqrt{P_T}\, u + w \tag{7}$$

i.e., the noise-free received signal is the same as the intended information symbol u scaled up by $\sqrt{P_T}$. Subsequently in this paper, we propose to choose $\mathcal{U} \subseteq \mathcal{M}(\mathbf{h})$,[6] and define the precoder map as in (6) and (5). With $\mathcal{U} \subseteq \mathcal{M}(\mathbf{h})$ it is clear that the information rate depends on $\mathcal{M}(\mathbf{h})$. In the next section, we give a more detailed characterization of $\mathcal{M}(\mathbf{h})$.

III. Characterization of $\mathcal{M}(\mathbf{h})$

We characterize $\mathcal{M}(\mathbf{h})$ through a series of intermediate results. First, we define the maximum and minimum absolute value of any complex number in $\mathcal{M}(\mathbf{h})$.

$$M(\mathbf{h}) \triangleq \max_{\Theta=(\theta_1,\cdots,\theta_N)\,,\,\theta_i\in[-\pi,\pi)} \left| \frac{\sum_{i=1}^{N} h_i e^{j\theta_i}}{\sqrt{N}} \right| \ , \ m(\mathbf{h}) \triangleq \min_{\Theta=(\theta_1,\cdots,\theta_N)\,,\,\theta_i\in[-\pi,\pi)} \left| \frac{\sum_{i=1}^{N} h_i e^{j\theta_i}}{\sqrt{N}} \right| \tag{8}$$

Lemma 1: If $z \in \mathcal{M}(\mathbf{h})$ then so does $ze^{j\phi}$ for all $\phi \in [-\pi, \pi)$.

[5] $\mathcal{U} \subseteq \mathcal{M}(\mathbf{h})$ implies that the information symbol alphabet must be chosen adaptively with $\mathbf{h}$. Therefore the receiver must be informed about the newly chosen $\mathcal{U}$, every time it changes. However, we shall see in Section III that the set $\mathcal{M}(\mathbf{h})$ is the interior of a "doughnut" shaped region in the 2-dimensional complex-plane and can therefore be fully characterized with only two non-negative real numbers (the inner and the outer radius of the doughnut). Hence, the TX only needs to inform the receiver about these two numbers every time $\mathbf{h}$ changes.

[6] For $\mathcal{U} \not\subseteq \mathcal{M}(\mathbf{h})$, it may be possible to consider a precoder map which satisfies (5) for $u \in \mathcal{M}(\mathbf{h})$, and for any $u \notin \mathcal{M}(\mathbf{h})$ finds the phase angle vector which minimizes the non-zero energy of the residual/error term $\left(\frac{\sum_{i=1}^{N} h_i e^{j\theta_i}}{\sqrt{N}} - u\right)$. However, even with such an error-minimizing precoder, it has been observed via simulations that having $\mathcal{U} \not\subseteq \mathcal{M}(\mathbf{h})$ does not increase the achievable information rate compared to when $\mathcal{U} \subseteq \mathcal{M}(\mathbf{h})$.

Proof – Since $z \in \mathcal{M}(\mathbf{h})$, from (4) it follows that there exists a phase vector $\Theta^z = (\theta_1^z, \theta_2^z, \cdots, \theta_N^z)$ such that $z = \frac{\sum_{i=1}^N h_i e^{j\theta_i^z}}{\sqrt{N}}$. Consider the phase angle vector $\tilde{\Theta}^z = (\tilde{\theta}_1^z, \tilde{\theta}_2^z, \cdots, \tilde{\theta}_N^z)$ with $\tilde{\theta}_i^z = \theta_i^z + \phi$, $i = 1, 2, \cdots, N$. It now follows that, $ze^{j\phi} = e^{j\phi}\frac{\sum_{i=1}^N h_i e^{j\theta_i^z}}{\sqrt{N}} = \frac{\sum_{i=1}^N h_i e^{j(\theta_i^z+\phi)}}{\sqrt{N}} = \frac{\sum_{i=1}^N h_i e^{j\tilde{\theta}_i^z}}{\sqrt{N}} \in \mathcal{M}(\mathbf{h})$. ■

Essentially Lemma 1 shows that the set $\mathcal{M}(\mathbf{h})$ exhibits a circular symmetry in $\mathbb{C}$. The following two lemmas characterize $M(\mathbf{h})$ and $m(\mathbf{h})$.

Lemma 2:

$$M(\mathbf{h}) = \frac{\sum_{i=1}^N |h_i|}{\sqrt{N}} = \frac{\|\mathbf{h}\|_1}{\sqrt{N}}. \tag{9}$$

Proof – The proof essentially follows from the extended triangular inequality $\left|\sum_{i=1}^N h_i e^{j\theta_i}\right| \leq \sum_{i=1}^N |h_i|$ with equality achieved when $e^{j\theta_i} = \frac{h_i^*}{|h_i|}$, i.e., $\theta_i = -\arg(h_i)$. ■

Lemma 3:

$$m(\mathbf{h}) \leq \frac{\|\mathbf{h}\|_\infty}{\sqrt{N}} = \frac{\max_{i=1,\ldots,N}|h_i|}{\sqrt{N}}. \tag{10}$$

Proof – Let the absolute values of the components of $\mathbf{h}$ be ordered as $|h_{i_1}| \geq |h_{i_2}| \geq \ldots \geq |h_{i_N}|$. By choosing the phase angles to be $\theta_{i_k} = -\arg(h_{i_k})$ for odd k and $\theta_{i_k} = -(\arg(h_{i_k}) + \pi)$ for even k, for even N we have $\sum_{i=1}^N h_i e^{j\theta_i} = \sum_{k=1}^N h_{i_k} e^{j\theta_{i_k}} = \sum_{k=1}^{N/2}\left(|h_{i_{2k-1}}| - |h_{i_{2k}}|\right) \leq \sum_{k=1}^{N-1}\left(|h_{i_k}| - |h_{i_{k+1}}|\right) = |h_{i_1}| - |h_{i_N}| \leq |h_{i_1}| = \|\mathbf{h}\|_\infty$. Similarly, for odd N, we have $\sum_{i=1}^N h_i e^{j\theta_i} = \left[\sum_{k=1}^{(N-1)/2}\left(|h_{i_{2k-1}}| - |h_{i_{2k}}|\right)\right] + |h_{i_N}| \leq \left[\sum_{k=1}^{N-2}\left(|h_{i_k}| - |h_{i_{k+1}}|\right)\right] + |h_{i_N}| = |h_{i_1}| - |h_{i_{N-1}}| + |h_{i_N}| \leq |h_{i_1}| = \|\mathbf{h}\|_\infty$. The proof now follows from the definition of $m(\mathbf{h})$. ■

In Appendix A, for the i.i.d. Rayleigh fading channel, we analytically show that for any constant $c > 0$, $\lim_{N\to\infty} \text{Prob}\left(m(\mathbf{h}) \geq \frac{c\log(N)}{\sqrt{N}}\right) = 0$, which essentially means that for any arbitrarily small $\epsilon > 0$, there exists a corresponding integer $N(\epsilon, c)$ such that $\text{Prob}\left(m(\mathbf{h}) \geq \frac{c\log(N)}{\sqrt{N}}\right) \leq \epsilon$ for all $N \geq N(\epsilon, c)$. Basically, it means that for sufficiently large N, with very high probability $m(\mathbf{h}) \leq \frac{c\log(N)}{\sqrt{N}}$. Since $\frac{c\log(N)}{\sqrt{N}} \to 0$ as $N \to \infty$, it follows that with increasing N, $m(\mathbf{h})$ approaches 0 with high probability. A similar result has been stated in [14], where it has been shown that for large N, $\|\mathbf{h}\|_\infty = \max_i |h_i| = \mathbb{E}[|h_i|]O(\log(N))$. Numerical results for the i.i.d. Rayleigh fading channel have however revealed that, with increasing N, $m(\mathbf{h})$ goes to zero at a significantly faster rate than $\log(N)/\sqrt{N}$ (implying that the upper bound in (10) is not quite tight). We illustrate this fact in Fig. 2, where we plot the mean value of the ratio $m(\mathbf{h})/M(\mathbf{h})$ and its upper bound $\|\mathbf{h}\|_\infty/\|\mathbf{h}\|_1$ as a function of increasing N. For i.i.d. fading channels where the channel gains are bounded, i.e., $|h_i| \leq M$ $\forall i = 1, 2, \cdots, N$ for some constant M, it follows

that $\|\mathbf{h}\|_\infty$ is also bounded ($\|\mathbf{h}\|_\infty \leq M$) and hence $\|\mathbf{h}\|_\infty / \sqrt{N}$ will converge to 0 as $N \to \infty$. Since, $m(\mathbf{h}) \leq \|\mathbf{h}\|_\infty / \sqrt{N}$, it immediately follows that $m(\mathbf{h}) \to 0$ as $N \to \infty$.[7] For the single-path only DLOS channel with $|h_1| = \cdots = |h_N|$, it can be shown that for any $N \geq 2$ and any $\mathbf{h}$, $m(\mathbf{h}) = 0$. (With $\theta_i = \frac{2\pi(i-1)}{N} - \arg(h_i), i = 1, 2, \ldots, N$, it is clear that $\sum_i h_i e^{j\theta_i} = 0$.)

The next theorem characterizes the set $\mathcal{M}(\mathbf{h})$.

Theorem 1:

$$\mathcal{M}(\mathbf{h}) = \Big\{ z \mid z \in \mathbb{C}\,,\, m(\mathbf{h}) \leq |z| \leq M(\mathbf{h}) \Big\}. \tag{11}$$

Proof – Let

$$(\theta_1^\star, \theta_2^\star, \cdots, \theta_N^\star) \triangleq \underset{\theta_i \in [-\pi, \pi)\,,\, i=1,2,\ldots,N}{\arg \min} \left| \frac{\sum_{i=1}^N h_i e^{j\theta_i}}{\sqrt{N}} \right| \tag{12}$$

Consider the single variable function

$$f(t) \triangleq \left| \frac{\sum_{i=1}^N h_i e^{j\theta_i(t)}}{\sqrt{N}} \right|^2 \;,\; t \in [0,1] \tag{13}$$

where the functions $\theta_i(t)\,,\, i = 1, 2, \ldots, N$ are defined as

$$\theta_i(t) \triangleq (1-t)\theta_i^\star - t \arg(h_i) \;,\; t \in [0,1]. \tag{14}$$

Note that $f(t)$ is a differentiable function of t, and therefore it is continuous for all $t \in [0,1]$. Also from (12), Lemma 2 and (8) it follows that

$$f(0) = m(\mathbf{h})^2 \;\;,\;\; f(1) = M(\mathbf{h})^2 \tag{15}$$

Since $f(t)$ is continuous, it follows that for any non-negative real number c with $m(\mathbf{h})^2 \leq c^2 \leq M(\mathbf{h})^2$, there exists a value of $t = t' \in [0,1]$ such that

$$f(t') = c^2. \tag{16}$$

Let

$$z' \triangleq \frac{\sum_{i=1}^N h_i e^{j\theta_i(t')}}{\sqrt{N}}. \tag{17}$$

From the definition of $\mathcal{M}(\mathbf{h})$ in (4) it is clear that $z' \in \mathcal{M}(\mathbf{h})$. From (16), (17) and (13) it follows that

$$|z'| = \sqrt{f(t')} = c. \tag{18}$$

Therefore, we have shown that for any non-negative real number $c \in [m(\mathbf{h})\,,\, M(\mathbf{h})]$, there exists a complex number having modulus c and belonging to $\mathcal{M}(\mathbf{h})$.

Further, from Lemma 1, we already know that the set $\mathcal{M}(\mathbf{h})$ is circularly symmetric, and therefore all complex numbers with modulus c belong to $\mathcal{M}(\mathbf{h})$. Since the choice of $c \in [m(\mathbf{h})\,,\, M(\mathbf{h})]$ was arbitrary, any complex number with modulus in the interval $[m(\mathbf{h})\,,\, M(\mathbf{h})]$ belongs to $\mathcal{M}(\mathbf{h})$. ■

[7]We conjecture that $m(\mathbf{h}) \to 0$ as $N \to \infty$ even if the i.i.d. channel gain distribution has *unbounded* support, though we do not have a rigorous proof of this statement.

A. The proposed precoder map $\Phi(u) = \Theta^u$

The proof of Theorem 1 is constructive and for a given $u \in \mathcal{U} \subseteq \mathcal{M}(\mathbf{h})$, it gives us a method to find the corresponding phase angle vector $\Theta^u = (\theta_1^u, \cdots, \theta_N^u)$ which satisfies (5). For a given $u \in \mathcal{U} \subseteq \mathcal{M}(\mathbf{h})$, we define the function $f_u(t) \stackrel{\Delta}{=} f(t) - |u|^2\ ,\ t \in [0,1]$ where $f(t)$ is given by (13). Using Newton-type methods or simple brute-force enumeration, we can find a $t = t_u$ satisfying $f_u(t_u) = 0$ (the existence of such a t_u is guaranteed by the constructive proof of Theorem 1). The phase angles which satisfy (5) are then given by $\theta_i^u = \theta_i(t_u) + \phi$ where $\theta_i(t)$ is given by (14), and ϕ is given by $e^{j\phi} = \frac{u\sqrt{N}}{\sum_{i=1}^N h_i e^{j\theta_i(t_u)}}$.

Yet another method to obtain Θ^u is to minimize the error norm function $e^u(\Theta) \stackrel{\Delta}{=} |u - \sum_{i=1}^N h_i e^{j\theta_i}/\sqrt{N}|^2$ w.r.t. Θ. For large N, it has been observed that, most local minima of the error norm function have small error norms, and therefore low-complexity methods like gradient descent can be used.[8] For very small $N = 2, 3$ there exist closed-form expressions for Θ^u as shown below.[9] From the expressions for the phase angle vector for very small N, and the existence of low-complexity gradient-descent type methods for large N, it is expected that the computational complexity of the proposed CE scheme would not be

[8]One method, that we have empirically found to have fast local minima convergence, is to sequentially update one phase angle at a time while keeping the others fixed in such a way that the objective function value $e^u(\Theta) \stackrel{\Delta}{=} |u - \sum_{i=1}^N h_i e^{j\theta_i}/\sqrt{N}|^2$ decreases with every update. Each update is a simple one-dimensional optimization problem, and since the convergence is fast, the order of complexity is expected to be the same as the MRT scheme, i.e., $O(N)$.

[9] For $N = 2$, $m(\mathbf{h}) = \big||h_1| - |h_2|\big|/\sqrt{2}$, and $M(\mathbf{h}) = (|h_1| + |h_2|)/\sqrt{2}$. For any $u \in \mathcal{M}(\mathbf{h})$, i.e., $m(\mathbf{h}) \le |u| \le M(\mathbf{h})$, the corresponding phase angle vector $\Theta^u = (\theta_1^u\ ,\ \theta_2^u)^T$ which satisfies (5) is given by

$$\theta_2^u = \cos^{-1}\left(\frac{|u|^2 + \frac{|h_2|^2}{2} - \frac{|h_1|^2}{2}}{\sqrt{2}|u||h_2|}\right) + \arg(u) - \arg(h_2)\ ,\ \theta_1^u = \arg\left(\frac{\sqrt{2}}{h_1}\Big(u - \frac{h_2}{\sqrt{2}}e^{j\theta_2^u}\Big)\right)$$

Note that there can be two possible solutions, since $\cos^{-1}(\cdot)$ can take two possible values in $[-\pi\ \pi)$.

For $N = 3$, $M(\mathbf{h}) = (|h_1| + |h_2| + |h_3|)/\sqrt{3}$, and $m(\mathbf{h})$ is given by

$$m(\mathbf{h}) = \begin{cases} \frac{\big||h_1| - |h_2|\big| - |h_3|}{\sqrt{3}} & |h_3| \le \big||h_1| - |h_2|\big| \\ 0 & \big||h_1| - |h_2|\big| \le |h_3| \le |h_1| + |h_2| \\ \frac{|h_3| - (|h_1| + |h_2|)}{\sqrt{3}} & |h_3| \ge |h_1| + |h_2| \end{cases}$$

For any $u \in \mathcal{M}(\mathbf{h})$, i.e., $m(\mathbf{h}) \le |u| \le M(\mathbf{h})$, the corresponding phase angle vector is $\Theta^u = (\theta_1^u\ ,\ \theta_2^u\ ,\ \theta_3^u)^T$, with θ_3^u satisfying

$$\frac{3|u|^2 + |h_3|^2 - (|h_1| + |h_2|)^2}{2\sqrt{3}|u||h_3|} \le \cos\big(\theta_3^u + \arg(h_3) - \arg(u)\big) \le \frac{3|u|^2 + |h_3|^2 - (|h_1| - |h_2|)^2}{2\sqrt{3}|u||h_3|}$$

Note that, θ_3^u can take infinitely many values. For a chosen θ_3^u, let $u_1 \stackrel{\Delta}{=} \sqrt{\frac{3}{2}}\Big(u - \frac{h_3 e^{j\theta_3^u}}{\sqrt{3}}\Big)$. The remaining angles are then given by

$$\theta_2^u = \cos^{-1}\left(\frac{|u_1|^2 + \frac{|h_2|^2}{2} - \frac{|h_1|^2}{2}}{\sqrt{2}|u_1||h_2|}\right) + \arg(u_1) - \arg(h_2)\ ,\ \theta_1^u = \arg\left(\frac{\sqrt{2}}{h_1}\Big(u_1 - \frac{h_2}{\sqrt{2}}e^{j\theta_2^u}\Big)\right)$$

significantly larger than the complexity of the MRT scheme when N is either very small or large.

When N is neither very small nor large (typically $3 < N \leq 10$), then the value of the error norm function may not be small at a significant fraction of local minima, which leads to poor performance of the gradient descent method. We therefore propose the following two-step algorithm for small N (i.e., $3 < N \leq 10$). In the first step, we find a value of $\Theta = \tilde{\Theta}^u$ such that $|u - \sum_{i=1}^{N} h_i e^{j\tilde{\theta}_i^u}/\sqrt{N}|^2$ is *sufficiently* small. This step ensures that with high probability, $\tilde{\Theta}^u$ is inside the region of attraction of the global minimum of the error norm function. In the second step, with this $\Theta = \tilde{\Theta}^u = (\tilde{\theta}_1^u, \cdots, \tilde{\theta}_N^u)$ as the initial vector, a simple gradient descent algorithm would then converge to the global minimum.

The first step of the proposed algorithm is based on the Depth-First-Search (DFS) technique. Basically, for a given u, we start with enumerating the possible values taken by $\tilde{\theta}_N^u$ such that (5) is satisfied with $\Theta^u = \tilde{\Theta}^u$. To satisfy (5), it is clear that $\tilde{\theta}_N^u$ must equivalently satisfy

$$u - \frac{h_N e^{j\tilde{\theta}_N^u}}{\sqrt{N}} = \sqrt{\frac{N-1}{N}} \frac{\sum_{i=1}^{N-1} h_i e^{j\tilde{\theta}_i^u}}{\sqrt{N-1}}. \tag{19}$$

Using Theorem 1, this is then equivalent to $(\sqrt{N}/\sqrt{N-1})(u - \frac{h_N e^{j\tilde{\theta}_N^u}}{\sqrt{N}}) \in \mathcal{M}((h_1, \cdots, h_{N-1})^T)$ i.e.

$$m(\mathbf{h}^{(N-1)}) \leq \sqrt{\frac{N}{N-1}} \Big| u - \frac{h_N e^{j\tilde{\theta}_N^u}}{\sqrt{N}} \Big| \leq M(\mathbf{h}^{(N-1)}) \tag{20}$$

where $\mathbf{h}^{(N-1)} \triangleq (h_1, \ldots, h_{N-1})^T$ and $m(\cdot), M(\cdot)$ are defined in (8). For example $M(\mathbf{h}^{(N-1)}) = \|\mathbf{h}^{(N-1)}\|_1/\sqrt{N-1}$. Equation (20) gives us an *admissible* set $I_N^u \subset [-\pi, \pi)$ to which $\tilde{\theta}_N^u$ must belong for (19) to be satisfied. We call this as the $k = 0$-th "depth" level of the proposed DFS technique.

Next, for a given value of $\tilde{\theta}_N^u \in I_N^u$, we go to the next "depth" level (i.e., $k = 1$) and find the set of admissible values for $\tilde{\theta}_{N-1}^u$. Essentially, at the k-th depth level, for a given choice of values of $(\tilde{\theta}_N^u, \tilde{\theta}_{N-1}^u, \ldots, \tilde{\theta}_{N-k+1}^u)$, with $\tilde{\theta}_{N-i+1}^u \in I_{N-i+1}^u, i = 1, \cdots, k$, we solve for the set of admissible values for $\tilde{\theta}_{N-k}^u$ such that (5) is satisfied with $\Theta^u = \tilde{\Theta}^u$. From Theorem 1, this set (i.e., I_{N-k}^u) is given by the values of $\tilde{\theta}_{N-k}^u$ satisfying

$$\sqrt{\frac{N-k-1}{N}}\, m(\mathbf{h}^{(N-k-1)}) \;\leq\; \Big| u^{(k)} - \frac{h_{N-k} e^{j\tilde{\theta}_{N-k}^u}}{\sqrt{N}} \Big| \;\leq\; \sqrt{\frac{N-k-1}{N}}\, M(\mathbf{h}^{(N-k-1)}) \tag{21}$$

where $u^{(k)} \triangleq (u - \sum_{i=1}^{k} \frac{h_{N-i+1}}{\sqrt{N}} e^{j\tilde{\theta}_{N-i+1}^u})$ and $\mathbf{h}^{(N-k-1)} \triangleq (h_1, \ldots, h_{N-k-1})^T$. If there exists no solution to (21) (i.e., I_{N-k}^u is empty), then the algorithm backtracks to the previous depth level i.e., $k-1$, and picks the next possible unexplored admissible value for $\tilde{\theta}_{N-k+1}^u$ from the set I_{N-k+1}^u. If there exists a solution to (21), then the algorithm simply moves to the next depth level, i.e., $k+1$. The algorithm terminates once it reaches a depth level of $k = N-1$ with a non-empty admissible set I_1. Since $u \in \mathcal{M}(\mathbf{h})$,

the algorithm is guaranteed to terminate (by Theorem 1). It can be shown that for depth levels less than $k = N-2$, the admissible set is generally an infinite set (usually a union of intervals in $\mathbb{R}$). Therefore, due to complexity reasons, at each depth level it is suggested to consider only a finite subset of values from the admissible set (e.g. values on a very fine grid), and terminate once the algorithm reaches a sufficiently high pre-defined depth level K with the current error norm $|u^{(K)}|$ below a pre-defined threshold. In the second step, a gradient descent algorithm starting with the initial vector $\Theta = (\tilde{\theta}^u_N, \ldots, \tilde{\theta}^u_{N-K+1}, 0, \ldots, 0)$, converges to the global minimum of the error norm function $e^u(\Theta)$. In terms of complexity, the first step of this two-step algorithm is expected to have a higher complexity when compared to the MRT scheme.

IV. The Doughnut Channel

Geometrically the set $\mathcal{M}(\mathbf{h})$ resembles a "doughnut" in the complex plane (see Theorem 1 and Fig. 3). With $\mathcal{U} \subseteq \mathcal{M}(\mathbf{h})$, and the precoder map in (6), we effectively have a "doughnut channel" (see (7))

$$y = \sqrt{P_T}\, u + w \quad , \quad m(\mathbf{h}) \leq |u| \leq M(\mathbf{h}) \ , \ w \sim \mathcal{CN}(0, \sigma^2) \tag{22}$$

which is a SISO AWGN channel where the information symbol u is constrained to belong to the "doughnut" set $\mathcal{M}(\mathbf{h})$. Therefore, with $\mathcal{U} \subseteq \mathcal{M}(\mathbf{h})$, it is clear that the capacity of the MISO channel with per-antenna CE inputs is equal to the capacity of the doughnut channel in (22), which is given by

$$C_{\text{donut}} = \sup_{p_u(\cdot)\,,\, u \in \mathcal{M}(\mathbf{h})} I(y; u) \tag{23}$$

where $I(y;u)$ denotes the mutual information between y and u, and $p_u(\cdot)$ is the p.d.f. of u. Due to the difficulty in deriving an exact expression for C_{donut}, we propose an appropriate lower and upper bound. The upper and lower bounds presented here will be used in Section VI to quantify the performance of the proposed CE scheme when compared to the average-only total power constrained MRT scheme.

A. An Achievable Information Rate for the Doughnut Channel (Lower Bound on Capacity)

For $N = 1$, the doughnut set contracts to a circle in the complex plane. In this case, capacity is achieved when the input u is uniformly distributed on this circle [7].

For $N > 1$, the information rate achieved with u *uniformly* distributed inside the doughnut set (i.e., the p.d.f. of u is $p_u^{\text{unif}}(z) = \frac{1}{\pi(M(\mathbf{h})^2 - m(\mathbf{h})^2)}$, $z \in \mathcal{M}(\mathbf{h})$) is given by

$$\begin{aligned} I(y;u)^{\text{unif}} \ &= \ I\Big(\frac{y}{\sqrt{P_T}}; u\Big) = h\Big(\frac{y}{\sqrt{P_T}}\Big) - h\Big(\frac{y}{\sqrt{P_T}} \mid u\Big) = h\Big(u + \frac{w}{\sqrt{P_T}}\Big) - h\Big(\frac{w}{\sqrt{P_T}}\Big) \\ &\geq \ \log_2(2^{h(u)} + 2^{h(w/\sqrt{P_T})}) - h(w/\sqrt{P_T}) = \log_2(1 + 2^{h(u) - h(w/\sqrt{P_T})}) \end{aligned} \tag{24}$$

where $h(s) \stackrel{\Delta}{=} -\int p_s(z)\log_2(p_s(z))dz$ denotes the differential entropy of the r.v. s ($p_s(\cdot)$ denotes the p.d.f. of s). The inequality in (24) follows from the Entropy Power Inequality (EPI) [15], which states that if $y = u + v$ where u and v are independent random variables, it holds that $2^{h(y)} \geq 2^{h(u)} + 2^{h(v)}$. Since u is uniformly distributed inside $\mathcal{M}(\mathbf{h})$, we have $h(u) = \log_2(\pi(M(\mathbf{h})^2 - m(\mathbf{h})^2))$. Using this in (24), we have the following lower bound[10]

$$C_{\text{donut}} \geq I(y;u)^{\text{unif}} \geq \log_2\left(1 + \frac{P_T}{\sigma^2}\frac{M(\mathbf{h})^2 - m(\mathbf{h})^2}{e}\right) \tag{25a}$$

$$C_{\text{donut}} \geq I(y;u)^{\text{unif}} \geq \log_2\left(1 + \frac{P_T}{\sigma^2}\frac{\|\mathbf{h}\|_1^2 - \|\mathbf{h}\|_\infty^2}{Ne}\right) \text{ (using Lemmas 2,3).} \tag{25b}$$

B. An Upper Bound on the Doughnut Channel Capacity

Let $s \stackrel{\Delta}{=} \frac{y}{\sqrt{P_T}}$, and let $p_s(\cdot)$ be its p.d.f. We now have

$$\begin{aligned} I(y;u) &= I(s;u) = h(s) - h(s\,|\,u) = -\int_{z\in\mathbb{C}} p_s(z)\log_2(p_s(z))dz \,-\, \log_2\left(\pi e\frac{\sigma^2}{P_T}\right) \\ &= -\int_{z\in\mathbb{C}} p_s(z)\log_2\left(\frac{p_s(z)}{g(z)}\right)dz - \int_{z\in\mathbb{C}} p_s(z)\log_2(g(z))dz \,-\, \log_2\left(\pi e\frac{\sigma^2}{P_T}\right) \\ &= -\mathrm{D}(p_s(.)||g(.)) - \int_{z\in\mathbb{C}} p_s(z)\log_2(g(z))dz \,-\, \log_2\left(\pi e\frac{\sigma^2}{P_T}\right) \\ &\leq -\int_{z\in\mathbb{C}} p_s(z)\log_2(g(z))dz \,-\, \log_2\left(\pi e\frac{\sigma^2}{P_T}\right) \end{aligned} \tag{26}$$

where $g(z)$ is some distribution function (i.e., $\int_{z\in\mathbb{C}} g(z)dz = 1$). Also, for any $z \in \mathbb{C}$, $g(z) > 0$. $\mathrm{D}(p_s(\cdot)||g(\cdot))$ denotes the Kullback-Leibler (KL) distance between the distributions $p_s(\cdot)$ and $g(\cdot)$. The last inequality in (26) follows from the fact that the KL distance between any two distributions is always non-negative. Since (26) holds for any distribution $g(\cdot)$, we aim to find a $g(\cdot)$ for which the integral $\int_{z\in\mathbb{C}} p_s(z)\log_2(g(z))dz$ can be computed in closed-form, and which also results in a sufficiently tight upper bound. We propose to use $g(z) = 2\beta e^{-\pi^3\beta^2|z|^4}$, $\beta > 0$. With this choice of $g(z)$ in (26), we have

$$I(y;u) \leq -\log_2(2\beta) + \pi^3\beta^2\log_2(e)\Big(M(\mathbf{h})^4 + 2\frac{\sigma^4}{P_T^2} + 4\frac{\sigma^2}{P_T}M(\mathbf{h})^2\Big) - \log_2(\pi e\frac{\sigma^2}{P_T}). \tag{27}$$

[10] With $N > 1$, a condition that is required for the usage of EPI to be valid is that $M(\mathbf{h}) > m(\mathbf{h})$, since otherwise the set $\mathcal{M}(\mathbf{h})$ has a zero Lebesgue measure leading to an undefined $h(u)$. From Lemma 2 and 3 it follows that the condition $\|\mathbf{h}\|_1 > \|\mathbf{h}\|_\infty$ implies $M(\mathbf{h}) > m(\mathbf{h})$. Since $\|\mathbf{h}\|_1 > \|\mathbf{h}\|_\infty$ holds for any $\mathbf{h}$ having more than one non-zero component, the required condition is met for most channel fading scenarios of practical interest.

Minimizing this upper bound w.r.t. the free parameter $\beta > 0$ gives

$$\begin{aligned} I(y;u) &\leq I^{(1)}\Big(\mathbf{h}, \frac{P_T}{\sigma^2}\Big) \ , \ I^{(1)}\Big(\mathbf{h}, \frac{P_T}{\sigma^2}\Big) \triangleq \frac{1}{2}\log_2\Big(\frac{\pi}{2e}\Big) + \frac{1}{2}\log_2\Big(M(\mathbf{h})^4\Big(\frac{P_T}{\sigma^2}\Big)^2 + 4M(\mathbf{h})^2\Big(\frac{P_T}{\sigma^2}\Big) + 2\Big) \\ &\leq \frac{1}{2}\log_2\Big(\frac{2\pi}{e}\Big) + \log_2\Big(1 + \frac{P_T}{\sigma^2}\frac{M(\mathbf{h})^2}{2}\Big) \end{aligned} \tag{28}$$

The bound in (28) is always valid irrespective of the distribution of u. Therefore it holds also for the distribution of u which maximizes $I(y;u)$ subject to $u \in \mathcal{M}(\mathbf{h})$.

Another upper bound to C_{donut} is given by the capacity of a MISO channel where the per-antenna *average-only* power is constrained to be P_T/N (i.e., $\mathbb{E}[|x_i|^2] = P_T/N \ , i = 1, \ldots, N$) for every channel realization $\mathbf{h}$. We shall subsequently refer to this constraint as PAPC. The capacity of the MISO channel under a PAPC constraint is given by [9][11]

$$C_{\text{PAPC}} = \log_2\Big(1 + \frac{P_T}{\sigma^2}M(\mathbf{h})^2\Big) \tag{29}$$

It is clear that, for a given total transmit power P_T, the PAPC constraint is much less restrictive than the CE constraint, and therefore $C_{\text{donut}} \leq C_{\text{PAPC}}$. We finally propose the following upper bound on C_{donut}

$$C_{\text{donut}} \leq I^{(2)}\Big(\mathbf{h}, \frac{P_T}{\sigma^2}\Big) \ , \ I^{(2)}\Big(\mathbf{h}, \frac{P_T}{\sigma^2}\Big) \triangleq \min\Big(I^{(1)}\Big(\mathbf{h}, \frac{P_T}{\sigma^2}\Big), C_{\text{PAPC}}\Big) \tag{30}$$

where $I^{(1)}\Big(\mathbf{h}, \frac{P_T}{\sigma^2}\Big)$ has been defined in (28).

V. On the capacity achieving input distribution for the doughnut channel

For the i.i.d. Rayleigh fading channel, i.i.d. fading channels with bounded channel gain and the DLOS channel, with high probability, the inner radius of the doughnut set $\mathcal{M}(\mathbf{h})$ shrinks to 0 as $N \to \infty$ (see Section III). This implies that, for large N the doughnut channel in (22) is essentially a *peak-input-amplitude only* limited SISO AWGN channel, with the per-channel use peak-amplitude constraint $|u| \leq M(\mathbf{h})$, i.e.

$$y = \sqrt{P_T}u + w \quad , \quad |u| \leq M(\mathbf{h}) \ , \ w \sim \mathcal{CN}(0, \sigma^2). \tag{31}$$

In the following, for large N we exploit this observation to propose a near-optimal capacity achieving input distribution ($p_u(\cdot)$) for the doughnut channel.

In [16], it has been shown that, for a peak-input-amplitude only constrained SISO AWGN channel, capacity is achieved with channel inputs that are *discrete* in *amplitude* and *uniform in phase* (DAUIP).

[11] For the PAPC constrained MISO channel, capacity is achieved by choosing u to be Gaussian distributed unit-energy symbols. For a given symbol u to be communicated, the optimal PAPC precoder transmits $\sqrt{P_T/N}(h_i^*/|h_i|)u$ from the i-th antenna.

In our notation, the information symbol $u \in \mathcal{U}_{\text{DAUIP}}^{L,\alpha}$, where $\mathcal{U}_{\text{DAUIP}}^{L,\alpha} = \cup_{l=1}^{L} \mathcal{U}_{\text{DAUIP}}^{l}$, with $L \in \mathbb{Z}^+$ and $\alpha = (\alpha_1, \alpha_2, \cdots, \alpha_L)^T$ ($\alpha_l \in (0\,,\,1]\,, \alpha_1 < \alpha_2 < \cdots < \alpha_L \leq 1$). $\mathcal{U}_{\text{DAUIP}}^{l}$ is given by

$$\mathcal{U}_{\text{DAUIP}}^{l} = \{v \in \mathbb{C} \mid |v| = \alpha_l M(\mathbf{h})\}. \tag{32}$$

Essentially, the DAUIP alphabet set is composed of L circles in $\mathbb{C}$ with the l-th circle having amplitude $\alpha_l M(\mathbf{h}), l = 1, 2, \ldots, L$. Furthermore, within a given circle, each point is equally likely (i.e., the phase is uniformly distributed). Let the probability that the information symbol u belongs to the l-th circle be denoted by $p_l\,,\, l = 1, 2, \ldots, L$, $\sum_l p_l = 1$. In [16], no closed-form expressions were given, neither for the capacity nor for the capacity achieving input (i.e., L, $\{\alpha_l\}$ and $\{p_l\}$). However, in [16], numerically it was shown that, at low peak-SNR (i.e., low $(P_T/\sigma^2)M(\mathbf{h})^2$ in our notation), it is optimal to use a single-amplitude DAUIP alphabet set with $L = 1\,,\, \alpha_1 = 1$, whereas with increasing peak-SNR, the number of circles in the optimal DAUIP alphabet also increases.

Based on the above discussion, for i.i.d. Rayleigh fading channel, i.i.d. fading channel with bounded channel gains and DLOS channels it can be concluded that, at large N, DAUIP inputs/alphabets are nearly optimal in terms of achieving the capacity of the doughnut channel/CE constrained MISO channel. In this paper, for a given N and P_T/σ^2, we numerically optimize the ergodic mutual information of the doughnut channel w.r.t. L and $\alpha_1 < \alpha_2 < \cdots < \alpha_L \leq 1$, i.e.

$$(L^\star, \alpha^\star) \;\triangleq\; \arg \max_{L \in \mathbb{Z}^+, 0 < \alpha_1 < \cdots < \alpha_L \leq 1} \mathbb{E}_{\mathbf{h}}[I(y;u)] \tag{33}$$

where, for a given (L, α), $u \in \mathcal{U}_{\text{DAUIP}}^{L,\alpha}$ and[12] $p_1 = p_2 = \cdots = p_L = 1/L$.[13] The numerical optimization in (33) can be performed off-line and therefore does not impact the online precoding complexity.

VI. Information rate comparison

With an average-only total transmit power constraint (ATPC), MRT with Gaussian information alphabet achieves the capacity of the single user Gaussian MISO channel, which is given by

$$C_{\text{ATPC}} = \log_2\left(1 + \|\mathbf{h}\|_2^2 \frac{P_T}{\sigma^2}\right). \tag{34}$$

[12]To be precise, $\mathcal{U}_{\text{DAUIP}}^{l}$ is chosen to consist of all complex numbers having magnitude $m(\mathbf{h}) + \alpha_l(M(\mathbf{h}) - m(\mathbf{h}))$. This choice is motivated by the fact that, for finite $N > 1$, even though $m(\mathbf{h})$ is small compared to $M(\mathbf{h})$, it is not exactly 0.

[13] In general, $p_1 = p_2 = \cdots = p_L = 1/L$ need not be optimal in terms of maximizing the ergodic mutual information. However, for the i.i.d. Rayleigh fading channel, we numerically observed that, in the practically interesting regime of low to moderate peak-SNR, it was optimal to have only a single circle, i.e., $L = 1$ (for which the trivial probability distribution is $p_1 = 1$). Also, designing practical channel codes for the doughnut channel would be much simpler when $p_1 = p_2 = \cdots = p_L = 1/L$.

Comparing (34) with (29) and (30) we have

$$C_{\text{donut}} < C_{\text{P}APC} \leq C_{\text{ATPC}} \tag{35}$$

For a desired information rate R, let the ratio of the total transmit power required under the per-antenna CE constraint to the total transmit power required under ATPC be referred to as the "power gap" between the proposed CE precoder and the MRT precoder (denoted by $P_{\text{gap}}^{\text{CE,MRT}}(R)$).[14]

$$P_{\text{gap}}^{\text{CE,MRT}}(R) \triangleq \frac{P^{\text{CE}}(R)}{P^{\text{MRT}}(R)} \tag{36}$$

where $P^{\text{CE}}(R)$ and $P^{\text{MRT}}(R)$ denote the total transmit power required by the CE scheme and the MRT scheme respectively, to achieve information rate R. We can similarly define the power gap between the proposed CE precoder and an optimal precoder operating under the PAPC constraint (denoted by $P_{\text{gap}}^{\text{CE,PAPC}}$). In the following, we investigate the power gap and the capacity ratios between the proposed CE precoder and the PAPC, MRT precoders, at low and high P_T/σ^2 (results are summarized in Table I).

A. Information Rate Comparison at Low $P_T M(\mathbf{h})^2/\sigma^2$

From the discussion in Section V we know that, at low $P_T M(\mathbf{h})^2/\sigma^2$ and large N, a single amplitude DAUIP information alphabet having complex symbols of magnitude $M(\mathbf{h})$ achieves near-capacity performance for the doughnut channel. Therefore, *in the low $P_T M(\mathbf{h})^2/\sigma^2$ regime, the capacity of the doughnut channel is roughly equal to that of a SISO non-fading AWGN channel (noise variance σ^2), where the input is constrained to have a constant envelope/amplitude of $M(\mathbf{h})\sqrt{P_T}$,* i.e.,

$$y = u + w \ , \ |u| = M(\mathbf{h})\sqrt{P_T} \, , \, w \sim \mathcal{CN}(0, \sigma^2). \tag{37}$$

The CE input constrained SISO AWGN channel in (37) was considered by Wyner in [7]. In [7], it was shown that for an average power only constrained AWGN channel (i.e., $y = u + w$), *using a CE input (instead of the capacity optimal Gaussian input) is almost information lossless for SNR $= \mathbb{E}[|u|^2]/\sigma^2 \leq 1$* .[15] Hence for $P_T M(\mathbf{h})^2/\sigma^2 \leq 1$ the capacity of the channel in (37) is roughly $\log_2(1 + P_T M(\mathbf{h})^2/\sigma^2)$. Using the capacity equivalence between the doughnut channel and the channel in (37), we have

$$C_{\text{donut}} \approx \log_2(1 + \frac{P_T}{\sigma^2} M(\mathbf{h})^2) \qquad \text{for } \frac{P_T}{\sigma^2} M(\mathbf{h})^2 \leq 1. \tag{38}$$

[14] In the following, we drop the argument R for notational brevity.

[15] See Eq. (14) and Fig. 2 in [7].

Further, comparing (38) with (29), we finally arrive at the conclusion that at low $(P_T/\sigma^2)M(\mathbf{h})^2 \leq 1$

$$C_{\text{donut}} \approx C_{\text{PAPC}} \qquad \text{for } \frac{P_T}{\sigma^2}M(\mathbf{h})^2 \leq 1. \tag{39}$$

Note that (39) holds for *any* channel realization $\mathbf{h}$. Using the capacity expressions (34) and (38), we can now conclude that,

$$P_{\text{gap}}^{\text{CE,MRT}} \approx \|\mathbf{h}\|^2 / M(\mathbf{h})^2 = \frac{\frac{\sum_{i=1}^N |h_i|^2}{N}}{\left(\frac{\sum_{i=1}^N |h_i|}{N}\right)^2} \geq 1 \quad \text{for } \frac{P_T}{\sigma^2}M(\mathbf{h})^2 \leq 1. \tag{40}$$

It is therefore clear that, at low SNR the power gap will be small when the channel gains from each antenna are similar in magnitude, and the power gap can be large when there is a large variation in the channel gains. For the single-path DLOS channel with $|h_1| = \cdots = |h_N|$, $P_{\text{gap}}^{\text{CE,MRT}} \approx 1$ for any $\mathbf{h}$. For i.i.d. Rayleigh fading channel and i.i.d. fading channels with bounded channel gains, using the law of large numbers and the Slutsky's Theorem, it can be shown that as $N \to \infty$

$$P_{\text{gap}}^{\text{CE,MRT}} \approx \frac{\frac{\sum_{i=1}^N |h_i|^2}{N}}{\left(\frac{\sum_{i=1}^N |h_i|}{N}\right)^2} \to_p \frac{\mathbb{E}[|h_i|^2]}{\left(\mathbb{E}[|h_i|]\right)^2} \tag{41}$$

where $\to_p$ denotes convergence in probability (w.r.t. the distribution of $\mathbf{h}$). For i.i.d. Rayleigh fading, this asymptotic (in N) power gap limit is $10\log_{10}(\mathbb{E}[|h_i|^2]/\left(\mathbb{E}[|h_i|]\right)^2) = 1.05$ dB.

As an illustrative numerical example, for the i.i.d. Rayleigh fading channel (with $\mathcal{CN}(0,1)$ distributed channel gains), in Figs. 4 and 5, we plot the ergodic information rate achieved under the ATPC, PAPC and CE input constraints for $N = 4$ and $N = 64$ respectively (as a function of P_T/σ^2). In both figures, for the proposed CE precoder with a DAUIP alphabet, we plot the ergodic information rate for different fixed values of L (i.e., L is fixed and does not change with P_T/σ^2 or with $\mathbf{h}$). For a fixed L and a given P_T/σ^2, we numerically maximize the achievable ergodic information rate as a function of $\alpha = (\alpha_1, \cdots, \alpha_L)$. Note that α only varies with P_T/σ^2, and does not vary with $\mathbf{h}$. For the special case of $L = 1$, we always choose $\alpha_1 = 1$. From the figures, it can be observed that, indeed at low $P_T M(\mathbf{h})^2/\sigma^2 \leq 1$ (corresponding to achievable rates $\log_2(1 + P_T M(\mathbf{h})^2/\sigma^2) \leq 1$ bpcu), as discussed previously, the information rate achieved by the proposed CE precoder with a single amplitude DAUIP information alphabet ($L = 1$) equals the MISO capacity under PAPC. This confirms (39), and also shows that the single amplitude DAUIP information alphabet ($L = 1$) is near-optimal for the proposed CE precoder at low $P_T M(\mathbf{h})^2/\sigma^2 \leq 1$. Note that at low $P_T M(\mathbf{h})^2/\sigma^2$, the ergodic information rate achieved with an information alphabet uniformly distributed inside the doughnut set, is strictly sub-optimal. Also, at low $P_T M(\mathbf{h})^2/\sigma^2 \leq 1$, the power gap

of the proposed CE precoder (DAUIP, $L = 1$) from the ATPC constrained MRT precoder is about 1.1 dB (close to the asymptotic power gap limit of 1.05 dB, see (41)). Note that, even with small $N = 4$, the CE-MRT power gap is close to the asymptotic limit.

Note that at low P_T/σ^2, we have $C_{\text{ATPC}} = \log_2(1 + (P_T/\sigma^2)\|\mathbf{h}\|^2) \approx (P_T/\sigma^2)\|\mathbf{h}\|^2 \log_2(e)$. Similarly, $C_{\text{donut}} \approx (P_T/\sigma^2)M(\mathbf{h})^2 \log_2(e)$. Therefore for low P_T/σ^2, we have

$$\frac{C_{\text{donut}}}{C_{\text{ATPC}}} \approx \frac{M(\mathbf{h})^2}{\|\mathbf{h}\|^2} \quad \text{for } \frac{P_T}{\sigma^2}M(\mathbf{h})^2 \ll 1. \tag{42}$$

which converges to $(\mathbb{E}[|h_i|])^2/\mathbb{E}[|h_i|^2]$ as $N \to \infty$ for the i.i.d. Rayleigh fading channel and i.i.d. fading channels with bounded channel gains. For the single-path DLOS channel this ratio is 1, i.e., per-antenna CE transmission is optimal even under ATPC. For the special case of $N = 1$, from [7] it follows that at low $P_T|h_1|^2/\sigma^2 \ll 1$, $C_{\text{donut}} \approx C_{\text{ATPC}}$.

B. Information Rate Comparison at High $P_T M(\mathbf{h})^2/\sigma^2$

In this section we derive lower and upper bounds to the CE-MRT power gap at high $P_T M(\mathbf{h})^2/\sigma^2$. Using the upper bound to the doughnut channel capacity in (28), it follows that in the asymptotic power limit as $P_T M(\mathbf{h})^2/\sigma^2 \to \infty$, the CE-MRT power gap is lower bounded as

$$P_{\text{gap}}^{\text{CE,MRT}} \geq \frac{2\|\mathbf{h}\|^2}{M(\mathbf{h})^2} \quad \text{for } \frac{P_T}{\sigma^2}M(\mathbf{h})^2 \gg 1. \tag{43}$$

For single-path DLOS channels, this lower bound on the CE-MRT power gap equals 3 dB, while for the i.i.d. Rayleigh fading channel and i.i.d. channels with bounded channel gains, it converges to $2\mathbb{E}[|h_i|^2]/(\mathbb{E}[|h_i|])^2$ as $N \to \infty$ (this is 4.06 dB for i.i.d. Rayleigh fading channel). Another interesting fact is that, at high $\frac{P_T}{\sigma^2}M(\mathbf{h})^2$, comparing the doughnut channel capacity upper bound in (28) and the PAPC capacity in (29) reveals that for *any* channel realization $\mathbf{h}$ and any N,

$$P_{\text{gap}}^{\text{CE,PAPC}} \geq 2 \quad \text{for } \frac{P_T}{\sigma^2}M(\mathbf{h})^2 \gg 1. \tag{44}$$

We now obtain an upper bound on the CE-MRT power gap. Using (25a) and (34) it follows that, for any $P_T M(\mathbf{h})^2/\sigma^2$ (not necessarily high), the CE-MRT power gap can be upper bounded as

$$P_{\text{gap}}^{\text{CE,MRT}} \leq \frac{1}{\kappa} \quad (\text{for all } \tfrac{P_T}{\sigma^2}M(\mathbf{h})^2), \ \kappa \triangleq \frac{M(\mathbf{h})^2 - m(\mathbf{h})^2}{e\|\mathbf{h}\|_2^2} = \frac{\left(\frac{\sum_i |h_i|}{N}\right)^2 - \frac{m(\mathbf{h})^2}{N}}{e\frac{\sum_i |h_i|^2}{N}} \tag{45}$$

For a single-path only DLOS channel with $|h_1| = \ldots = |h_N|$, for any $\mathbf{h}$ and any $N > 1$ it can be shown that $1/\kappa = e$ (since $m(\mathbf{h}) = 0$ for $N > 1$). With i.i.d. Rayleigh fading and i.i.d. fading channels with

bounded channel gains, as $N \to \infty$, using the law of large numbers and Slutsky's Theorem along with the fact that $m(\mathbf{h}) \to 0$ as $N \to \infty$ (see Section III),

$$\kappa \to_p \left(\mathbb{E}[|h_i|]\right)^2 / \, e\mathbb{E}[|h_i|^2] \tag{46}$$

Therefore, for the i.i.d. Rayleigh fading channel and i.i.d. fading channels with bounded channel gains, in the asymptotic limit as $N \to \infty$, combining (43), (45) and (46) we have,

$$2\frac{\mathbb{E}[|h_i|^2]}{(\mathbb{E}[|h_i|])^2} \;\leq\; P_{\text{gap}}^{\text{CE,MRT}} \;\leq\; e\frac{\mathbb{E}[|h_i|^2]}{(\mathbb{E}[|h_i|])^2} \quad \left(N \gg 1 \,,\; \frac{P_T}{\sigma^2} M(\mathbf{h})^2 \gg 1 \right) \tag{47}$$

Therefore, with sufficiently large N and high $P_T M(\mathbf{h})^2/\sigma^2$, the difference between the upper and the lower bounds on the CE-MRT power gap is $10\log_{10}(e/2) = 1.33$ dB *irrespective of the channel fading distribution* (as long as the channel gains are bounded). For i.i.d. Rayleigh fading, the asymptotic upper and lower bounds on the CE-MRT power gap are 5.4 and 4.1 dB respectively, see Fig. 5.[16] For the practically interesting low to moderate $P_T M(\mathbf{h})^2/\sigma^2$ regime, with DAUIP alphabets the CE-MRT power gap is usually lesser than its asymptotic lower bound. We illustrate this fact through Fig. 6, where we plot the ergodic information rate as a function of increasing P_T/σ^2 for the MRT and the proposed CE precoder (i.i.d. Rayleigh fading channel). The reported ergodic rate for the proposed CE precoder is with the proposed best DAUIP information alphabet in (33). It can be seen that with a properly chosen DAUIP information alphabet, the CE-MRT power gap is roughly 3.5 dB for a desired information rate of 3 bpcu. Also, the CE-MRT power gap is small even for $N = 2$, which makes CE transmission possible for conventional TX with few antennas.

We now investigate the ratio $C_{\text{donut}}/C_{\text{ATPC}}$ at high $P_T M(\mathbf{h})^2/\sigma^2$. For $N = 1$, it is known that, at large $P_T|h_1|^2/\sigma^2$ (i.e., large C_{ATPC}), capacity with a CE input is roughly *half* of the channel capacity under ATPC [7]. This fact is illustrated in Fig. 6, where, for $N = 1$ the channel capacity under CE transmission has a much smaller slope w.r.t. P_T/σ^2 as compared to the slope of the channel capacity under ATPC. For $N > 1$, using (25a), (34) and (35) it can be shown that

$$1 > \frac{C_{\text{donut}}}{C_{\text{ATPC}}} > \frac{I(y;u)^{\text{unif}}}{C_{\text{ATPC}}} \geq 1 - \frac{\log_2\left(\frac{1}{\kappa}\right)}{C_{\text{ATPC}}}. \tag{48}$$

[16] In Fig. 5, note that the power gap lower bound at a desired information rate of 3 bpcu is only 2 dB, as compared to the power gap lower bound limit of 4.1 dB. This is because, for a desired rate of 3 bpcu, the corresponding $P_T M(\mathbf{h})^2/\sigma^2$ is still not high enough for the asymptotic lower bound in (47) to be valid. A stronger result which can be seen by comparing (43) and (45) is that, for channels where $m(\mathbf{h}) \to 0$ as $N \to \infty$, at high $P_T M(\mathbf{h})^2/\sigma^2$ the upper to lower bound gap is 1.33 dB *for any* $\mathbf{h}$ (not limited to i.i.d. fading).

For the i.i.d. Rayleigh fading channel and i.i.d. fading channels with bounded channel gains, the convergence in (46) implies that, for any arbitrary $\epsilon > 0$, there exists an integer $N(\epsilon)$ such that with $N > N(\epsilon)$, the probability that a channel realization will have a value of $\kappa \geq \frac{(\mathbb{E}[|h_i|])^2}{e\mathbb{E}[|h_i|^2]} - \epsilon$ is greater than $1-\epsilon$. For single-path DLOS channels we already know that $\kappa = 1/e$ for $N > 1$. Compared to $N = 1$, with $N \gg 1$ and high $P_T M(\mathbf{h})^2/\sigma^2$, from (48) it follows that CE transmission can achieve an information rate *close* to the capacity C_{ATPC} under ATPC, since $1 - \frac{\log_2(1/\kappa)}{C_{\text{ATPC}}}$ is *close to* 1 (as C_{ATPC} is large, and κ is greater than a positive constant with high probability), i.e.

$$\frac{C_{\text{donut}}}{C_{\text{ATPC}}} \approx 1 \quad \text{for } N \gg 1 \ , \ \frac{P_T}{\sigma^2} M(\mathbf{h})^2 \gg 1. \tag{49}$$

This fact is illustrated through Fig. 4 and Fig. 5, where it can be seen that for both $N = 4$ and $N = 64$, the slope of the ergodic information rate achieved with per-antenna CE transmission (with information symbols uniformly distributed inside the doughnut set) is the same as the slope of the ergodic channel capacity under ATPC. Similar observations can be made from Fig. 6 with DAUIP alphabets. The intuitive reasoning for this observation is as follows. For $N = 1$, the doughnut set is a circle in the complex plane, due to which information symbols have the same amplitude and differ from each other only in the phase (i.e., they exploit only one degree of freedom for information transmission). In contrast, with $N > 1$, the doughnut set includes all complex numbers with amplitude in the range $[m(\mathbf{h}) \, , \, M(\mathbf{h})]$, which implies that information symbols can vary in both phase and amplitude (exploiting both degrees of freedom).

VII. Achievable Array Power Gain

For a desired rate R and a given precoding scheme, with N antennas, the *array power gain* achieved by this scheme is defined to be the factor of reduction in the total transmit power required to achieve a fixed rate of R bpcu, when the number of TX antennas is increased from 1 to N. Under ATPC, with N antennas the MRT precoder achieves an array power gain of (using (34))

$$G_N^{\text{MRT}}(R) = \frac{\sum_{i=1}^{N} |h_i|^2}{|h_1|^2} \tag{50}$$

which is $O(N)$ for i.i.d. fading and DLOS. With CE transmission, using the R.H.S of (25a) as the achievable information rate, the array power gain achieved with N antennas is given by

$$G_N^{\text{CE}}(R) = N \, \frac{G_2^{\text{CE}}(R)}{2} \, \frac{\left\{ \left\{ \sum_{i=1}^{N} |h_i|/N \right\}^2 - m(\mathbf{h})^2/N \right\}}{\left\{ \left\{ \sum_{i=1}^{2} |h_i|/2 \right\}^2 - (|h_1| - |h_2|)^2/4 \right\}} \tag{51}$$

where $G_2^{\text{CE}}(R)$ is the array power gain achieved with only 2 antennas and depends only on h_1 and h_2. From (51), it is clear that $G_N^{\text{CE}}(R)$ is $O(N)$ for i.i.d. Rayleigh fading, i.i.d. fading with bounded channel

gains and DLOS (for i.i.d. Rayleigh fading and i.i.d. fading with bounded channel gains, $\sum_i |h_i|/N \rightarrow_p \mathbb{E}[|h_i|]$ and $m(\mathbf{h})^2/N \rightarrow_p 0$ as $N \rightarrow \infty$). Therefore, for practical fading scenarios like i.i.d. Rayleigh fading, i.i.d. fading with bounded channel gains and DLOS, *an $O(N)$ array power gain can indeed be achieved even with per-antenna CE transmission.*

This conclusion is validated in Fig. 7, where we plot the minimum P_T/σ^2 required by the CE, MRT, and the PAPC precoder to achieve an ergodic information rate of $R = 3$ bpcu. For all precoders, it is observed that, at sufficiently large N, the required P_T/σ^2 reduces by roughly 3 dB with every doubling in the number of TX antennas. This confirms the fact that, an $O(N)$ array power gain can be achieved even with per-antenna CE transmission. The minimum required P_T/σ^2 is also tabulated in Table II.

VIII. Outage probability under per-antenna CE transmission

In scenarios where the channel coherence time is much longer than the end-to-end delay requirements and where a constant data throughput rate is desired, we are faced with the possibility of an outage, wherein the channel capacity is less than the desired information rate. The outage probability under ATPC is defined as $P_{\text{out}}^{\text{ATPC}}(R, P_T/\sigma^2) \triangleq \text{Prob}(C_{\text{ATPC}} \leq R) = \text{Prob}(\|\mathbf{h}\|^2 \leq (2^R - 1)\sigma^2/P_T)$ where R is the desired constant information rate. To have a low outage probability, one needs to increase the total transmit power P_T. With large N, due to the increased degrees of freedom in the r.v. $\|\mathbf{h}\|^2$ (χ^2 distributed with $2N$ degrees of freedom for i.i.d. Rayleigh distributed channel gains) it is clear that, *under ATPC the slope of the outage probability for the MISO channel w.r.t. P_T/σ^2 increases with increasing N* (on a log-log plot this slope in the asymptotic limit of $P_T/\sigma^2 \rightarrow \infty$ is commonly known as the "diversity" order). Further, a higher slope at large N implies that less extra P_T would be required to achieve a fixed decrease in the desired outage probability. However, it is not clear, as to whether the above conclusion is valid even under per-antenna CE transmission.

Using the proposed upper and lower bound to C_{donut} (see Sections IV-A and IV-B) we can derive lower and upper bounds to the outage probability of the proposed CE precoder. The outage probability of the proposed CE precoder is given by

$$\begin{aligned} P_{\text{out}}^{\text{CE}}(R, P_T/\sigma^2) &\triangleq \text{Prob}(C_{\text{donut}} \leq R) \\ &\geq \text{Prob}\Big(I^{(2)}\Big(\mathbf{h}, \frac{P_T}{\sigma^2}\Big) \leq R\Big) \end{aligned} \tag{52}$$

where the second inequality follows from the upper bound to C_{donut} in (30), since $\{I^{(2)}\Big(\mathbf{h}, \frac{P_T}{\sigma^2}\Big) \leq R\}$ implies that $\{C_{\text{donut}} \leq R\}$. Similarly, by using the lower bound to C_{donut} in (25a) we get the following upper bound on $P_{\text{out}}^{\text{CE}}(R, P_T/\sigma^2)$

$$P_{\text{out}}^{\text{CE}}(R, P_T/\sigma^2) \;\; \leq \;\; \text{Prob}\Big(\log_2 \Big(1 + \frac{P_T}{\sigma^2}\frac{M(\mathbf{h})^2 - m(\mathbf{h})^2}{e}\Big) \leq R\Big) \tag{53}$$

The diversity order achieved is defined as

$$d_{\text{out}}^{\text{CE}} \;\; \triangleq \;\; \lim_{\frac{P_T}{\sigma^2}\to\infty} \frac{-\log(P_{\text{out}}^{\text{CE}}(R, P_T/\sigma^2))}{\log(P_T/\sigma^2)} \tag{54}$$

In Appendix B we analytically show that $d_{out}^{CE} \geq (N-1)$ for the i.i.d. $\mathcal{CN}(0,1)$ Rayleigh fading channel. This result is tight for large N, since the maximum achievable diversity order is N.

We support the above conclusion through Fig. 8, where we plot the upper and lower bounds on the outage probability of the proposed CE precoder as a function of P_T/σ^2 for $N = 2, 4, 16, 64$ (i.i.d. Rayleigh fading). The bounds on the right hand side of (52) and (53), have been computed through simulations. It can be seen that for a constant desired rate of $R = 2$ bpcu, the slope of the outage probability curves increase with increasing N.

IX. Overall Improvement in Power Efficiency by using CE Transmission

On one hand, with CE transmission we improve the power efficiency by enabling the use of highly power-efficient amplifiers, but at the same time, restricting the per-antenna channel inputs to CE (since highly power-efficient amplifiers are generally non-linear) requires extra transmit power (compared to Gaussian inputs) to achieve a fixed desired information rate. If this extra transmit power is significantly smaller than the improvement in power efficiency gained by using highly power-efficient amplifiers, then it is clear that using per-antenna CE transmission will lead to an overall gain in power efficiency.

Motivated by the above discussion, for a TX with N antennas, compared to using highly linear and power-inefficient amplifiers with Gaussian inputs (MRT precoder), the overall gain in power efficiency by using highly power-efficient amplifiers with per-antenna CE inputs is given by $\rho \triangleq \frac{\text{PAE}_{\text{non-linear}}}{\text{PAE}_{\text{linear}}} \,/\, P_{\text{gap}}^{\text{CE,MRT}}$ where $\text{PAE}_{\text{non-linear}}$ and $\text{PAE}_{\text{linear}}$ denote the power-efficiency of non-linear and linear power amplifiers respectively.[17] For a highly linear power amplifier, $\text{PAE}_{\text{linear}} \approx 0.15 - 0.25$, whereas a highly power-efficient but non-linear amplifier has $\text{PAE}_{\text{non-linear}} \approx 0.7 - 0.85$ [17]. As an illustrative example, with

[17]For an RF power amplifier, the power efficiency is the ratio of the total RF power radiated to the total amplifier input power.

$\text{PAE}_{\text{linear}} = 0.2$ and $\text{PAE}_{\text{non-linear}} = 0.8$, using analytical results on $P_{\text{gap}}^{\text{CE,MRT}}$ (see Section VI), it follows that in single-path DLOS and i.i.d. Rayleigh fading channels *it is indeed beneficial to use per-antenna CE inputs with highly power-efficient amplifiers* ($P_{\text{gap}}^{\text{CE,MRT}} \leq 4\ (6\text{dB})$ implies that $\rho > 1$). At practically interesting low to moderate values of $P_T M(\mathbf{h})^2/\sigma^2$, for i.i.d. Rayleigh fading channels ρ varies from 4.95 dB (at rates below 1 bpcu) to 2.5 dB (at an information rate of 3 bpcu).

X. Conclusions and Future Work

In this paper, we derived an achievable rate for a single-user Gaussian MISO channel under the constraint that the signal transmitted from each antenna has a constant envelope. We showed that for i.i.d. Rayleigh fading channels, i.i.d. fading channels with bounded channel gains and DLOS channels, even with the stringent per-antenna CE constraint, an $O(N)$ array power gain can be achieved with N antennas. Also, compared to the average-only total transmit power constrained channel, the extra total transmit power required under the CE constraint to achieve a desired rate (i.e., power gap), is shown to be bounded and small. We conjecture that these results hold true for a much broader class of fading channels, and are not limited to i.i.d. Rayleigh fading, i.i.d. fading channels with bounded channel gains and DLOS channels. We are currently extending the results in this paper to the multi-user setting, see [18].

References

[1] A. Fehske, G. Fettweis, J. Malmodin and G. Biczok, "The global footprint of mobile communications: the ecological and economic perspective," *IEEE Communications Magazine*, pp. 55-62, August 2011.

[2] D. N. C. Tse, *Fundamentals of Wireless Communications, Cambridge University Press*, 2005.

[3] F. Rusek, D. Persson, B. K. Lau, E. G. Larsson, O. Edfors, F. Tufvesson and T. L. Marzetta, "Scaling up MIMO: opportunities and challenges with very large arrays," to appear in *IEEE Signal Processing Magazine.*

[4] T. L. Marzetta, "Non-cooperative cellular wireless with unlimited numbers of base station antennas," *IEEE. Trans. on Wireless Communications*, pp. 3590–3600, vol. 9, no. 11, Nov. 2010.

[5] R. Zhang and S. Cui, "Cooperative interference management with MISO beamforming," *IEEE. Trans. on Signal Processing*, pp. 5450–5458, vol. 58, no. 10, Oct. 2010.

[6] V. Mancuso and S. Alouf, "Reducing costs and pollution in cellular networks," *IEEE Communications Mag.*, pp. 63-71, August 2011.

[7] A. D. Wyner, "Bounds on communication with polyphase coding," *Bell Sys. Tech. Journal*, pp. 523-559, vol. 45, Apr. 1966.

[8] D. P. Palomar, "Unified framework for linear MIMO transceivers with shaping constraints," *IEEE Communication Letters*, pp. 697-699, vol. 8, no. 12, Dec. 2004.

[9] M. Vu, "MISO capacity with per-antenna power constraint," *IEEE Trans. on Communications*, pp. 1268-1274, vol. 59, no. 5, May 2011.

[10] U. G. Schuster, G. Durisi, H. Bölcskei and H. V. Poor, "Capacity Bounds for Peak-Constrained Multiantenna Wideband Channels," *IEEE Transactions on Communications*, pp. 2686-2696, vol. 57, no. 9 Sept. 2009.

[11] W. Yu and T. Lan, "Transmitter optimization for the multi-antenna downlink with per antenna power constraints," *IEEE Trans. Sig. Proc.*, pp. 2646-2660, vol. 55, June 2007.

[12] K. Karakayali, R. Yates, G. Foschini and R. Valenzuela, "Optimum Zero-forcing Beamforming with Per-antenna Power Constraints," *IEEE International Symposium on Information Theory ISIT'07*, pp. 101-105, Nice, France, June 2007.

[13] S. Shi, M. Schubert and H. Boche, "Per-antenna power constrained rate optimization for multiuser MIMO systems," *in proc. of International ITG Workshop on Smart Antennas, WSA'2008*, pp. 270-277, Feb. 2008.

[14] M. Sharif and B. Hassibi, "On the capacity of MIMO broadcast channels with partial side information," *IEEE Transactions on Information Theory*, pp. 506-522, vol. 51, no. 2, Feb. 2005.

[15] S. Verdu and D. Guo, "A simple proof of the entropy-power inequality," *IEEE Transactions on Information Theory*, pp. 2165-2166, vol. 52, no. 5, May 2006.

[16] S. Shamai (Shitz) and I. Bar-David, "The capacity of average and peak-power-limited quadrature Gaussian channels," *IEEE Transactions on Information Theory*, pp. 1060-1071, vol. 41, no. 4 July 1995.

[17] S. C. Cripps, *RF Power Amplifiers for Wireless Communications*, Artech Publishing House, 1999.

[18] S. K. Mohammed and E. G. Larsson, "Constant envelope precoding for power-efficient downlink wireless communication in multi-user MIMO systems using large antenna arrays," *in Proc. IEEE ICASSP 2012*, Kyoto, Japan, March 2012. `arXiv:1111.1191v1`

[19] M. Abramowitz and I. A. Stegun *Handbook of Mathematical Functions with Formulas, Graphs and Mathematical Tables*, National Bureau of Standards (USA), Applied Mathematics Series 55, ninth printing, 1970.

[20] H. A. David, *Order Statistics*, John Wiley and Sons, 1970.

APPENDIX A
ON THE ORDER OF $m(\mathbf{h})$ AS $N \to \infty$

Before discussing the main result, we make some definitions. For a random channel vector $\mathbf{h} = (h_1, h_2, \cdots, h_N)^T$, let $Z_i \stackrel{\Delta}{=} |h_i|^2$. Further, let $Z_{(i)}\,, i = 1, 2, \cdots, N$ be defined to be the i-th smallest value among $Z_1, \cdots, Z_N$. Therefore, we have $0 \leq Z_{(1)} \leq Z_{(2)} \leq \cdots \leq Z_{(N)} < \infty$.

Theorem 2: For an i.i.d. $\mathcal{CN}(0,1)$ Rayleigh fading channel, for any constant $c > 0$

$$\lim_{N\to\infty} \text{Prob}\Big(m(\mathbf{h}) \geq \frac{c\log(N)}{\sqrt{N}}\Big) = 0 \tag{55}$$

where $m(\mathbf{h})$ has been defined in (8).

Proof – It suffices to prove that

$$\lim_{N\to\infty} \text{Prob}\Big(m(\mathbf{h}) \leq \frac{c\log(N)}{\sqrt{N}}\Big) = 1 \tag{56}$$

Further, since $m(\mathbf{h}) \leq \frac{\|\mathbf{h}\|_\infty}{\sqrt{N}} = \frac{\max_{i=1,\ldots,N}|h_i|}{\sqrt{N}}$ (Lemma 3), it suffices to show that

$$\lim_{N\to\infty} \text{Prob}\Big(\|\mathbf{h}\|_\infty \leq c\log(N)\Big) = 1 \tag{57}$$

In terms of the newly defined random variables above, this is equivalent to proving that

$$\lim_{N\to\infty} \text{Prob}\Big(Z_{(N)} \;\leq\; c^2\log^2 N\Big) \;=\; 1 \tag{58}$$

Due to i.i.d. $\mathcal{CN}(0,1)$ Rayleigh fading, the random variables $Z_i, i = 1, 2, \cdots, N$ are i.i.d. exponentially distributed with mean value 1. Therefore

$$\begin{aligned}\text{Prob}\Big(Z_{(N)} \;\leq\; c^2\log^2 N\Big) \;&=\; \prod_{i=1}^{N}\text{Prob}\Big(Z_i \;\leq\; c^2\log^2 N\Big) \;=\; \prod_{i=1}^{N}\Big(1 \;-\; e^{-c^2\log^2 N}\Big)\\ &=\; \Big(1 \;-\; e^{-c^2\log^2 N}\Big)^N \;=\; \Big(1 \;-\; \frac{1}{N^{c^2\log N}}\Big)^N.\end{aligned} \tag{59}$$

We next show that

$$\lim_{N\to\infty} \log \text{Prob}\Big(Z_{(N)} \;\leq\; c^2\log^2 N\Big) \;=\; \lim_{N\to\infty} N\log\Big(1-\frac{1}{N^{c^2\log N}}\Big) = 0 \tag{60}$$

from which (58) follows immediately. To prove (60), note that for any $c > 0$ and all $N > 2$, $N^{c^2\log N} > 1$. Further, using the inequality $\log(1-x) \leq -x$ for $0 \leq x < 1$ [19], for $N > 2$ we have

$$N\log\Big(1-\frac{1}{N^{c^2\log N}}\Big) \;\leq\; -\frac{N}{N^{c^2\log N}} \tag{61}$$

Using (61) we have

$$\lim_{N\to\infty} N\log\Big(1-\frac{1}{N^{c^2\log N}}\Big) \;\leq\; -\lim_{N\to\infty}\frac{N}{N^{c^2\log N}} = 0. \tag{62}$$

Using the inequality $\log(1-x) \geq -x/(1-x)$ for $0 \leq x < 1$ [19], for $N > 2$ we have

$$N\log\Big(1-\frac{1}{N^{c^2\log N}}\Big) \;\geq\; -\frac{N}{N^{c^2\log N}}\frac{1}{1 \;-\; e^{-c^2\log^2 N}} \tag{63}$$

which implies that

$$\lim_{N\to\infty} N\log\Big(1-\frac{1}{N^{c^2\log N}}\Big) \;\geq\; -\lim_{N\to\infty}\frac{N}{N^{c^2\log N}}\frac{1}{1 \;-\; e^{-c^2\log^2 N}} = 0. \tag{64}$$

Combining (64) and (62) proves (60) which completes the proof.

APPENDIX B

DIVERSITY ANALYSIS FOR THE OUTAGE PROBABILITY OF THE PROPOSED CE PRECODER

Using the lower bound on C_{donut} in (25b), an upper bound on the outage probability is given by

$$P_{\text{out}}^{\text{CE}}(R, P_T/\sigma^2) \;=\; \text{Prob}(C_{\text{donut}} \leq R) \;\leq\; \text{Prob}\Big(\log_2\Big(1+\frac{P_T}{\sigma^2}\frac{\|\mathbf{h}\|_1^2 - \|\mathbf{h}\|_\infty^2}{Ne}\Big) \leq R\Big) \tag{65}$$

In terms of the new random variables defined at the beginning of Appendix A, we have

$$\|\mathbf{h}\|_1^2 - \|\mathbf{h}\|_\infty^2 \;=\; \Big(\sum_{i=1}^{N}\sqrt{Z_{(i)}}\Big)^2 \;-\; Z_{(N)} \;\geq\; \sum_{i=1}^{N-1} Z_{(i)}. \tag{66}$$

Using this fact in (65), we have

$$P_{\text{out}}^{\text{CE}}(R, P_T/\sigma^2) \;\leq\; \text{Prob}\Big(\log_2 \Big(1 + \frac{P_T}{\sigma^2}\frac{\sum_{i=1}^{N-1} Z_{(i)}}{Ne}\Big) \leq R\Big) \tag{67}$$

Let us define random variables

$$Y_i \;\stackrel{\Delta}{=}\; (N-i+1)\,(Z_{(i)} \,-\, Z_{(i-1)}) \;\; i = 1, 2, \cdots, N. \tag{68}$$

Note that $Y_1 \stackrel{\Delta}{=} NZ_{(1)}$. For the i.i.d. $\mathcal{CN}(0,1)$ Rayleigh fading channel, it is known that $Y_i \in [0\,,\,\infty)\,,\, i = 1, 2, \cdots, N$ are i.i.d. exponentially distributed random variables with mean 1 (see section 2.7, page 17 in [20]). From the definition above, it immediately follows that

$$\sum_{i=1}^{N-1} Y_i \;=\; Z_{(N-1)} \,+\, \sum_{i=1}^{N-1} Z_{(i)} \tag{69}$$

which implies that

$$\sum_{i=1}^{N-1} Z_{(i)} \;\geq\; \frac{1}{2}\sum_{i=1}^{N-1} Y_i \tag{70}$$

since Y_i and $Z_{(i)}$ are non-negative random variables. Using (70) in (67) we have

$$P_{\text{out}}^{\text{CE}}(R, P_T/\sigma^2) \;\leq\; \text{Prob}\Big(\log_2 \Big(1 + \frac{P_T}{\sigma^2}\frac{\sum_{i=1}^{N-1} Y_i}{2Ne}\Big) \leq R\Big) \;=\; \text{Prob}\Big(\sum_{i=1}^{N-1} Y_i \,\leq\, \frac{2eN(2^R-1)}{P_T/\sigma^2}\Big) \tag{71}$$

Since, the event $\sum_{i=1}^{N-1} Y_i \,\leq\, \frac{2eN(2^R-1)}{P_T/\sigma^2}$ implies that each $Y_i \,\leq\, \frac{2eN(2^R-1)}{P_T/\sigma^2}$, we further have

$$P_{\text{out}}^{\text{CE}}(R, P_T/\sigma^2) \;\leq\; \text{Prob}\Big(Y_i \,\leq\, \frac{2eN(2^R-1)}{P_T/\sigma^2} \;,\; i = 1, 2, \cdots, N-1\Big) \tag{72}$$

Since Y_i are i.i.d. exponentially distributed, the right hand side in the above can be further simplified to

$$P_{\text{out}}^{\text{CE}}(R, P_T/\sigma^2) \;\leq\; \prod_{i=1}^{N-1} \text{Prob}\Big(Y_i \,\leq\, \frac{2eN(2^R-1)}{P_T/\sigma^2}\Big) \;=\; \Big(1 \,-\, e^{-\frac{2eN(2^R-1)}{P_T/\sigma^2}}\Big)^{N-1} \tag{73}$$

The diversity order achieved by the outage probability therefore satisfies

$$d_{\text{out}}^{\text{CE}} \;\stackrel{\Delta}{=}\; \lim_{\frac{P_T}{\sigma^2}\to\infty} \frac{-\log(P_{\text{out}}^{\text{CE}}(R, P_T/\sigma^2))}{\log(P_T/\sigma^2)} \;\geq\; (N-1) \lim_{\frac{P_T}{\sigma^2}\to\infty} \frac{-\log\Big(1 \,-\, e^{-\frac{2eN(2^R-1)}{P_T/\sigma^2}}\Big)}{\log\Big(\frac{P_T}{\sigma^2}\Big)} \tag{74}$$

where we have used (73) for the inequality. Using the identity

$$\lim_{x\to 0} \frac{\log(1-e^{-cx})}{\log x} \;=\; 1 \;\; (c > 0) \tag{75}$$

with $x = \sigma^2/P_T$ and $c = 2eN(2^R-1) \,> 0$, we have

$$\lim_{\frac{P_T}{\sigma^2}\to\infty} \frac{-\log\Big(1 \,-\, e^{-\frac{2eN(2^R-1)}{P_T/\sigma^2}}\Big)}{\log\Big(\frac{P_T}{\sigma^2}\Big)} \;=\; 1 \tag{76}$$

which then proves that

$$d_{\text{out}}^{\text{CE}} \;\geq\; (N-1) \tag{77}$$

TABLE I

CAPACITY RATIOS/POWER GAP OF CE TRANSMISSION W.R.T. MRT AND PAPC TRANSMISSION

	$N \gg 1$				$N = 1$	
	$\frac{P_T}{\sigma^2} M(\mathbf{h})^2 \ll 1$		$\frac{P_T}{\sigma^2} M(\mathbf{h})^2 \gg 1$		$\frac{P_T}{\sigma^2} \lvert h_1 \rvert^2 \ll 1$	$\frac{P_T}{\sigma^2} \lvert h_1 \rvert^2 \gg 1$
	i.i.d. Rayleigh fading, i.i.d. fading channels with bounded channel gains	DLOS	i.i.d. Rayleigh fading, i.i.d. fading channels with bounded channel gains	DLOS		
$P_{\text{gap}}^{\text{CE,MRT}}$ (dB)	$10 \log_{10}(\frac{\mathbb{E}[\lvert h_i \rvert^2]}{(\mathbb{E}[\lvert h_i \rvert])^2})$	0	$\geq 3 + 10 \log_{10}(\frac{\mathbb{E}[\lvert h_i \rvert^2]}{(\mathbb{E}[\lvert h_i \rvert])^2})$ $\leq 4.3 + 10 \log_{10}(\frac{\mathbb{E}[\lvert h_i \rvert^2]}{(\mathbb{E}[\lvert h_i \rvert])^2})$	≥ 3 ≤ 4.3	0	∞
$P_{\text{gap}}^{\text{CE,PAPC}}$ (dB)	0	0	≥ 3 ≤ 4.3	≥ 3 ≤ 4.3	0	∞
$\frac{C_{\text{donut}}}{C_{\text{ATPC}}}$	$\frac{(\mathbb{E}[\lvert h_i \rvert])^2}{\mathbb{E}[\lvert h_i \rvert^2]}$	1	1	1	1	$\frac{1}{2}$
$\frac{C_{\text{donut}}}{C_{\text{PAPC}}}$	1	1	1	1	1	$\frac{1}{2}$

TABLE II

SIGNAL-TO-NOISE-RATIO P_T/σ^2 (DB) REQUIRED TO ACHIEVE AN ERGODIC RATE OF 3 BPCU (I.I.D. $\mathcal{CN}(0,1)$ RAYLEIGH FADING)

	N=1	N=2	N=3	N=4	N=8	N=16	N = 32	N = 64
MRT (ATPC)	10.2	6.4	4.3	2.9	-0.4	-3.5	-6.5	-9.5
PAPC	10.2	6.9	5.0	3.7	0.6	-2.5	-5.5	-8.6
CE (best DAUIP)	14.3	9.8	7.6	6.2	3.1	0	-3.0	-6.0
CE (UNIF)	14.3	10.4	9.0	8.2	5.0	1.8	-1.3	-4.4

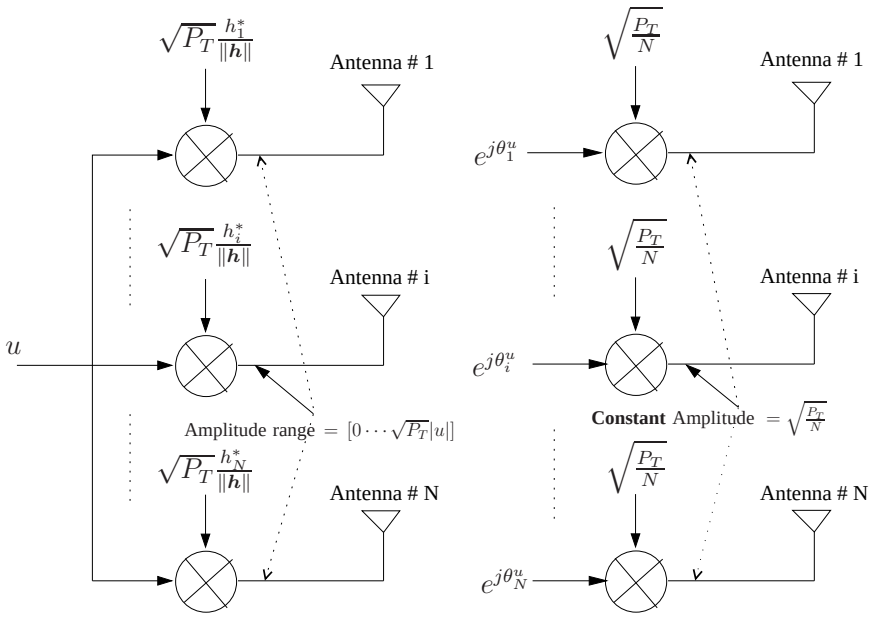

(a) MRT (b) CE

Fig. 1. Maximum Ratio Transmission (MRT) versus per-antenna Constant Envelope (CE) constrained transmission, for a given average total transmit power constraint of P_T. $\mathbf{h} = (h_1, \cdots, h_N)^T$ is the vector of complex channel gains.

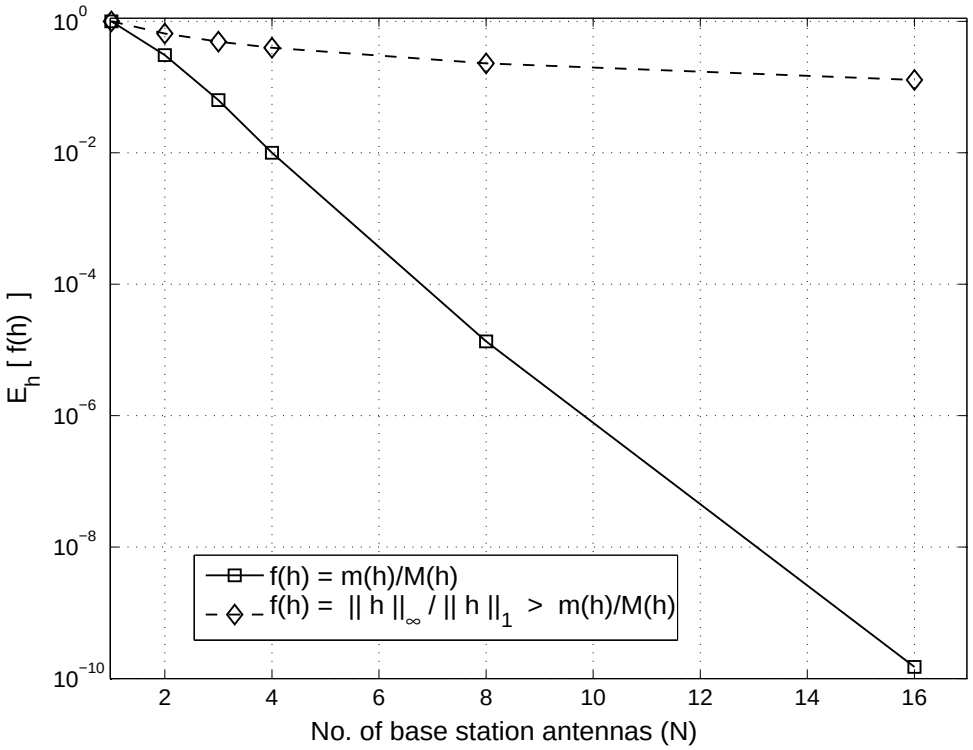

Fig. 2. Mean value of the ratio $m(\mathbf{h})/M(\mathbf{h})$ as a function of increasing N, for i.i.d. $\mathcal{CN}(0,1)$ Rayleigh fading. We calculate $m(\mathbf{h})$ in (8) using an iterative gradient descent type method.

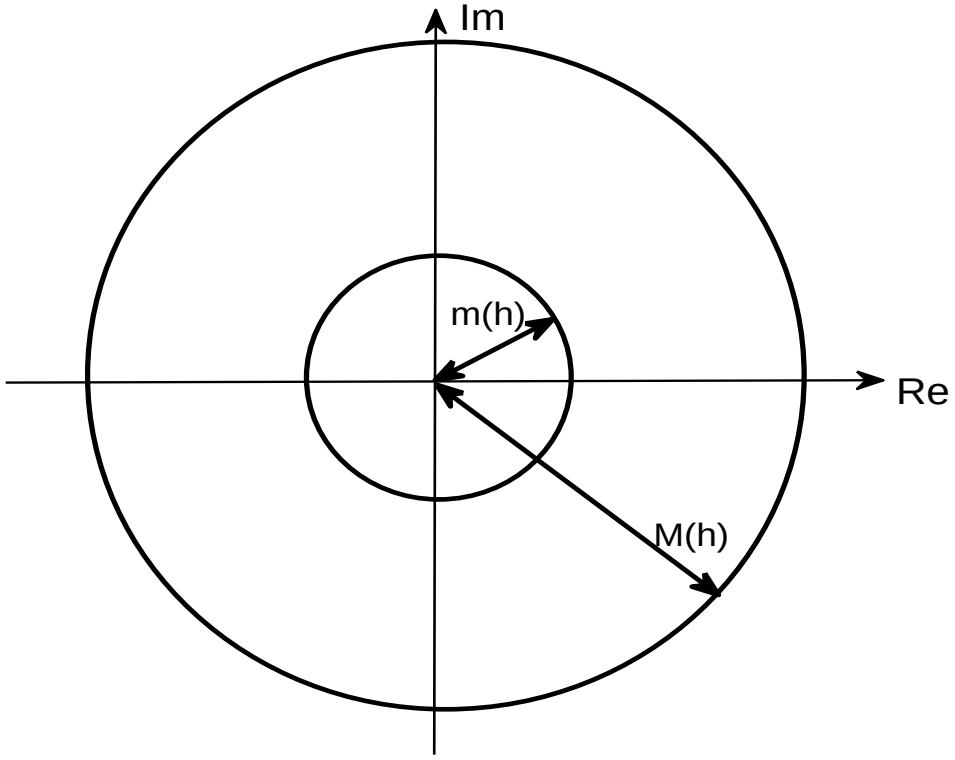

Fig. 3. The doughnut set $\mathcal{M}(\mathbf{h})$ in the complex plane. $\mathcal{M}(\mathbf{h})$ contains all points in the "doughnut" shaped region between the outer and the inner circles of radius $M(\mathbf{h})$ and $m(\mathbf{h})$ respectively.

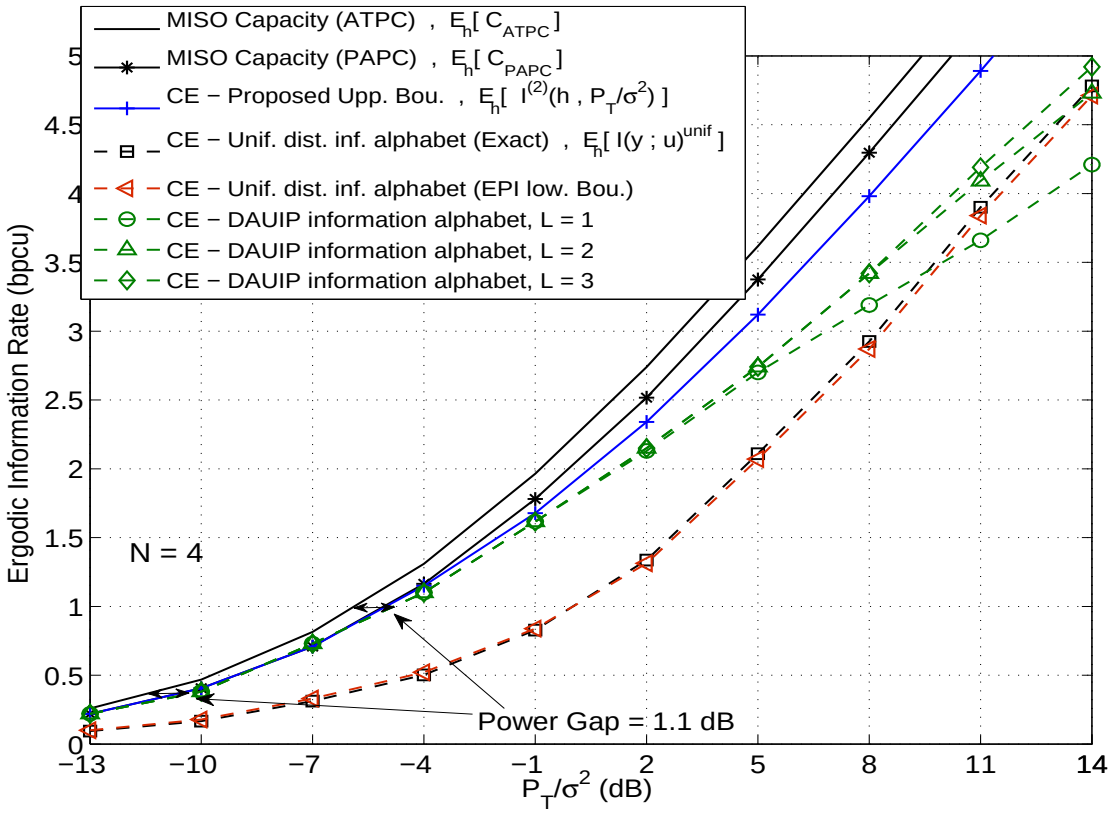

Fig. 4. Ergodic information rate vs. P_T/σ^2, for i.i.d. $\mathcal{CN}(0,1)$ Rayleigh fading and $N = 4$.

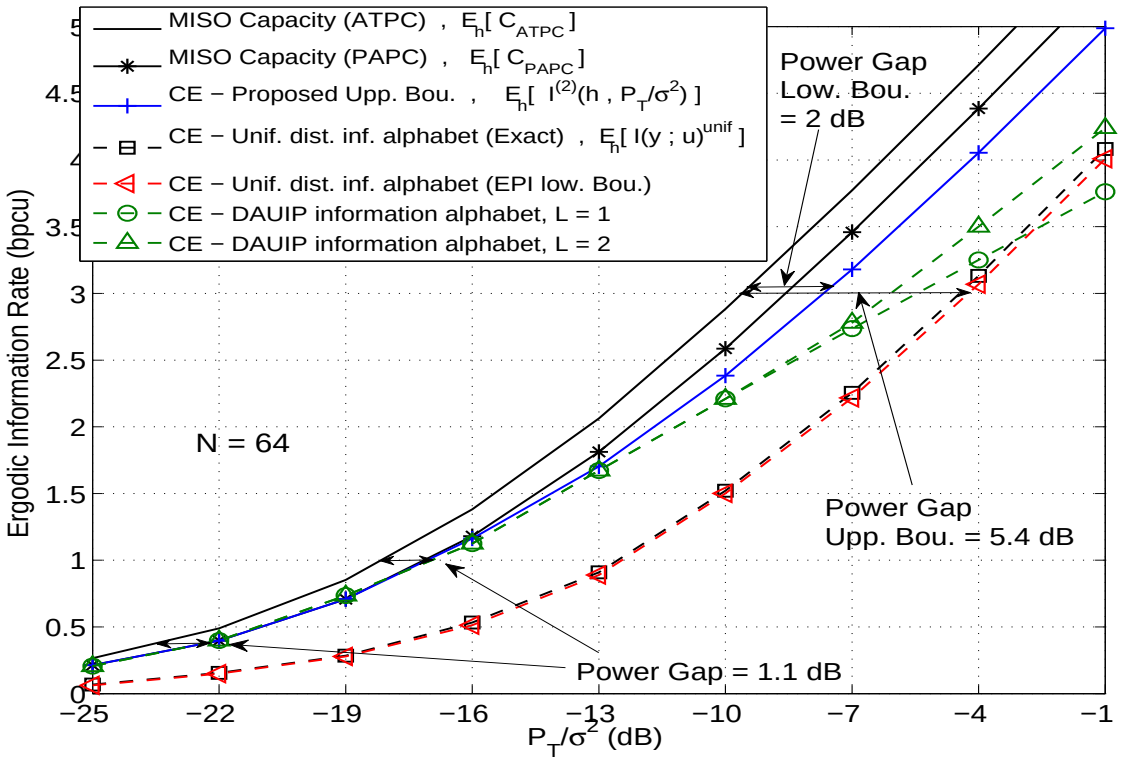

Fig. 5. Ergodic information rate vs. P_T/σ^2 for i.i.d. $\mathcal{CN}(0,1)$ Rayleigh fading and $N = 64$.

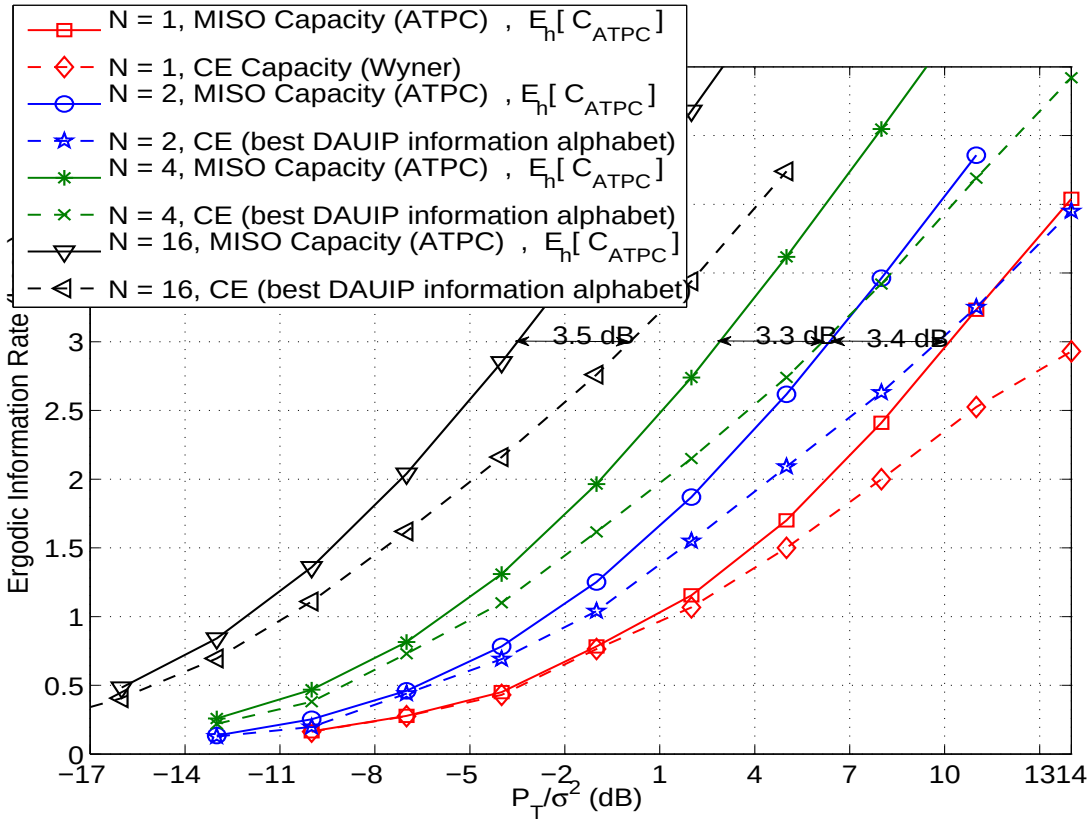

Fig. 6. Ergodic information rate vs. P_T/σ^2 for i.i.d. $\mathcal{CN}(0,1)$ Rayleigh fading and $N = 1, 2, 4, 16$.

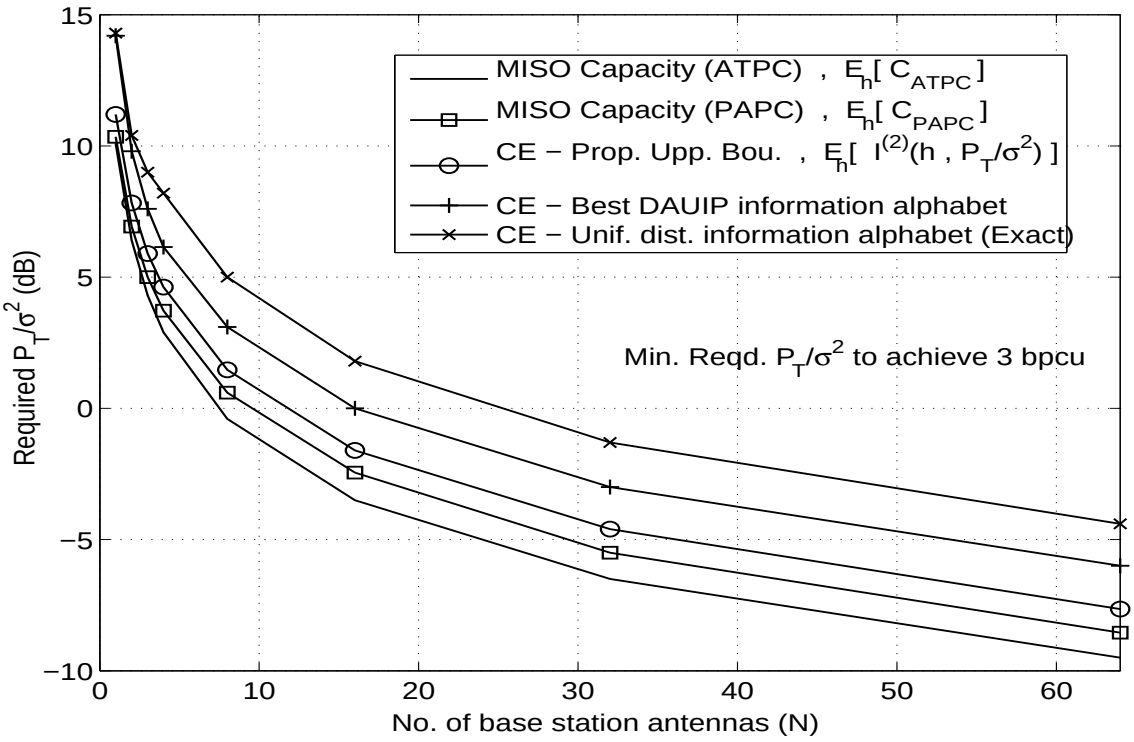

Fig. 7. Minimum P_T/σ^2 required to achieve an ergodic information rate of 3 bpcu as a function of the number of antennas N, for i.i.d. $\mathcal{CN}(0,1)$ Rayleigh fading.

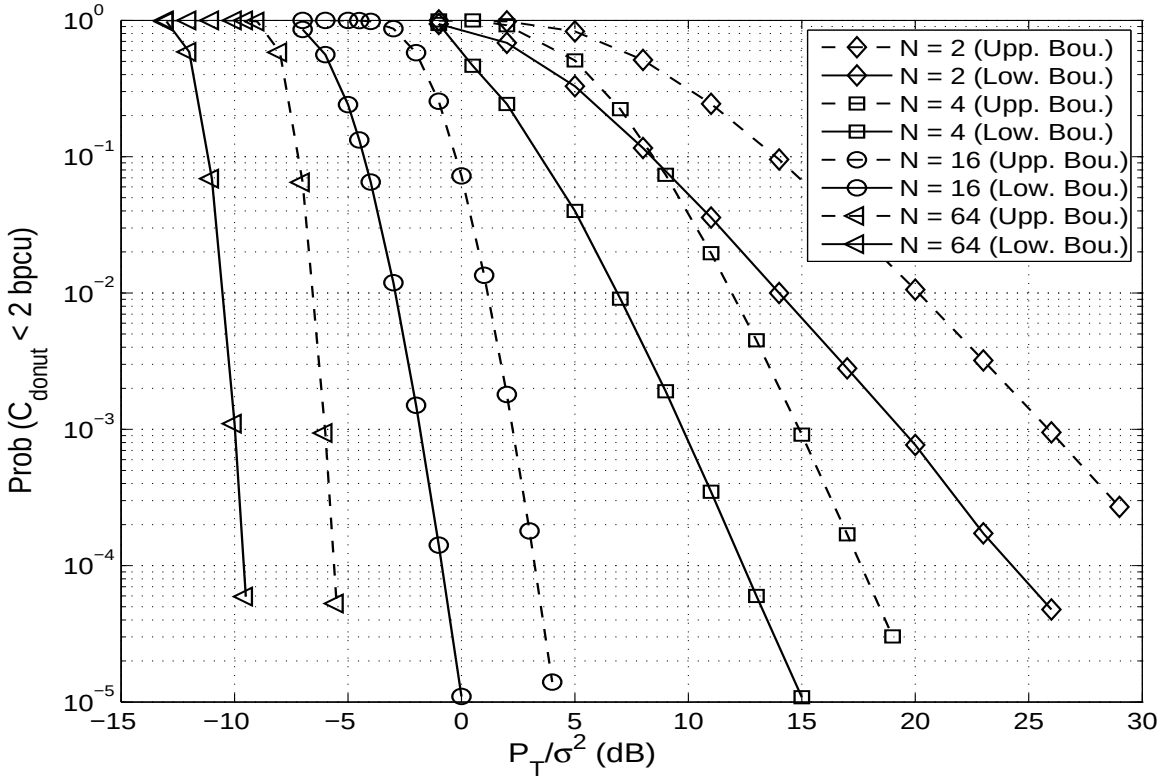

Fig. 8. Upper and lower bounds on the outage probability of the proposed CE precoder at rate 2 bpcu, as a function of P_T/σ^2, for i.i.d. $\mathcal{CN}(0,1)$ Rayleigh fading.